Molecular Quantum States at Dissociation

Edited by

Rita Prosmiti
Jonathan Tennyson
David C. Clary

Molecular Quantum States at Dissociation

Edited by

Rita Prosmiti[1]
Jonathan Tennyson[1]
David C. Clary[2]

[1]Department of Physics & Astronomy,
[2]Department of Chemistry,
University College London,
Gower Street, London WC1E 6BT,
United Kingdom

Suggested Dewey classification: 541.39

ISBN 0-9522736-5-9

Published by

Collaborative Computational Project
on Heavy Particle Dynamics (CCP6),
Daresbury Laboratory,
Daresbury,
Warrington, WA4 4AD,
United Kingdom

R. Prosmiti, J. Tennyson, D. C. Clary (eds.)
Molecular Quantum States at Dissociation

Preface

This booklet was produced as a result of the CCP6 Workshop on "Molecular Quantum States at Dissociation", which was held in the Chemistry Department of University College London on 29th and 30th June, 1998. Each speaker in the workshop was invited to prepare a brief review of work in their own area, with references to their own and related work. The articles are designed to provide a good introduction to the field for workers outside it and an update for those more directly involved.

Collaborative Computation Project 6 (CCP6) on Heavy Particle Dynamics started in 1980. For nearly two decades it has comprised scientists from two schools: those working on bound state problems and those studying collision dynamics. Of course some of the more ambitious members of CCP6 attempted to be in both schools at once! However I welcome this workshop as quantum states at dissociation: high lying bound states and resonances, actually represents the point where the two schools of study meet. The topic is thus at the very heart of CCP6 activity.

Quantum states of at dissociation have come under increasing experimental scrutiny. Carrington's group at Southampton has laid down much of the experimental challenge in this field by recording high resolution spectra of molecular at their dissociation limit. This work has stimulated much of the theoretical work reported in the booklet. Hutson *et al.* report their progress in assigning spectra of ionic complexes; Prosmiti *et al.* give the latest in the long running theoretical struggle to interpret the many resonances observed in the near-dissociation photodissociation spectrum of H_3^+ originally recorded by Carrington's group in the early eighties. It is generally accepted that the resonances in the H_3^+ are due to rotationally excited states trapped behind an angular momentum barrier. Kozin and Roberts report on the use classical considerations to analyse the highly rotationally excited states of H_3^+. The struggle to understand the photodissociation spectrum of H_3^+ has prompted several groups to develop new techniques to compute bound and quasibound molecular states. Taylor and then Mandelshtam report on their development of signal processing techniques developed for this and other problems. One system Mandelshtam and Taylor have applied their methods to in NO_2, a notoriously difficult molecule to treat because the large amount of vibronic coupling. Grebenshchikov *et al.* consider how quasibound states or resonances alter the dissociation dynamics of this molecule.

Hernández *et al.* also treat dissociation dynamics, this time of the Van der Waals cluster $HeBr_2$. Wright and Hutson analyse the bound vibrational

states of argon Van der Waals trimer. Rotational motion can only be included exactly in bound state or scattering calculations at considerable computational cost. Bowman studies rotational motion for resonances and whether this can be reliably modelled using approximate models. Zhang discusses the use of time-dependent methods for treating resonances, while Truhlar considers non-adiabatic coupling effects on resonance lifetimes. He finds that none of the current semiclassical models for treating electronically non-adiabatic processes are reliable. Finally Miller suggests how this problem might be resolved.

Although the Workshop's primary sponsor was CCP6, it also received support from the Chemical Reactions and Energy Exchange Processes computing consortium, ChemReact. This grouping, which was loosely based about the membership of CCP6 with the additional members from CCP1 ('The Electronic Structure of Molecules'), was formed in 1995 to exploit the then newly purchased, massively parallel Cray-T3D supercomputer located at the Edinburgh Parallel Computing Centre. Results derived by the ChemReact consortium feature in this booklet. Finally all the editors would like to thank Dr Paul Dando and Dr Ismanuel Rabadán for their considerable help with the organisation of the workshop and the production of this booklet.

Jonathan Tennyson
University College London

What is CCP6?

Jeremy M. Hutson
Department of Chemistry, University of Durham, South Road, Durham, DH1 3LE, UK

CCP6 is Collaborative Computational Project No. 6 of the United Kingdom Engineering and Physical Sciences Research Council (EPSRC). There are a number of CCPs, mostly in physics and chemistry, with interests ranging from electron scattering to protein crystallography. CCP6 is interested in "Heavy Particle Dynamics", which includes:

- atomic collisions, especially nonadiabatic and electron transfer collisions;
- elastic and inelastic molecular scattering;
- reactive molecular collisions;
- photodissociation and photoionisation processes;
- time-dependent quantum mechanics;
- bound states of molecules, especially in the presence of wide-amplitude motion.

A wide variety of techniques is used to study these problems, including quantum-mechanical, semiclassical and classical dynamical methods.

The CCPs were originally formed to provide scientific direction for the national supercomputer facilities in the UK, and to coordinate scientific activities using the supercomputers. They thus have a dual role, advising on the requirements for new supercomputers and the directions that the supercomputer facilities should take in the future, and coordinating scientific work by different groups in the United Kingdom.

CCP6's activities are coordinated by a "Working Group" made up of about 20 research group leaders from dynamics groups around the country. They are supported by "Advisers", who are experts in fields that overlap with CCP6, but whose main research thrust is in other areas. There are also one or two overseas representatives on the CCP6 working group.
Information about CCP6 is available on the World Wide Web at URL
http://www.dci.clrc.ac.uk/Activity.asp?CCP6

CCP6's activities fall into several categories:

1. Specialist conferences

CCP6 organises about two conferences per year. These are sometimes on specialist computational subjects, such as "Parallel Processing", and sometimes on more general subjects of interest to the CCP6 community, such as "Fitting Molecular Potential Energy Surfaces" or "Photodissociation Dynamics". The conferences serve to transfer technical expertise between researchers using similar computational methods, and thus prevent people "reinventing the wheel", as well as allowing people to communicate their new scientific results.

2. Program Library

CCP6 maintains a library of programs for performing calculations in all the subject areas listed above. The programs are obtained from the authors, sometimes modified to run efficiently on the supercomputers currently available, and made generally available free of charge to the UK scientific community. Where possible, full documentation is also made available.
Details of the program library are available on the World Wide Web from a link at the CCP6 site described above.

3. Research Programme

CCP6 provides funding for research workers to travel to other sites for collaborative computational research, especially research that will lead to enhancements of CCP6 programs. It also occasionally pays for overseas researchers to visit the UK to assist in installing new programs on the supercomputers in the UK.

CCP6 also usually employs one or two postdoctoral research assistants, to work on projects of general interest to the CCP6 community. In the past, CCP6 post-docs have worked on inelastic and reactive molecular scattering, on non-adiabatic atomic collisions and on the development of computational tools for least-squares fitting to obtain potential energy surfaces. The current CCP6 post-doc is working on developing a new reactive scattering package.

4. CCP6 Newsletter

The CCP6 Newsletter is published about once per year, and exists mostly to spread information about CCP6 conferences and the work of CCP6 members outside the CCP6 community itself. It publishes conference announcements, short informal articles describing research in CCP6's areas of interest, and announcements of new programs (and new versions of programs) available through CCP6.

The CCP6 Workshop Series

CCP6 regularly organises specialist workshops in its areas of interest. The workshops are designed to bring together the leading specialists in the field for a meeting that usually lasts two or three days. The focus is usually on technical issues to do with how calculations are actually carried out, and is thus rather different from most other scientific meetings.

Each participant at a CCP6 Workshop is invited to prepare a brief review of their field, with references to their own and related work, and the resulting articles are published in the CCP6 Workshop Series.

PREVIOUS BOOKLETS IN THE CCP6 WORKSHOP SERIES

1. M. M. Law, J. M. Hutson and A. Ernesti (editors), "Fitting Molecular Potential Energy Surfaces" (1993). ISBN 0-9522736-0-8.
2. G. G. Balint-Kurti and M. M. Law (editors), "Photodissociation Dynamics" (1994). ISBN 0-9522736-1-6.
3. M. S. Child and M. M. Law (editors), "Intramolecular dynamics in the frequency and time domains" (1995). ISBN 0-9522736-2-4.
4. A. Ernesti, J. M. Hutson and C. F. Roche (editors), "Molecular Collisions in the Atmosphere" (1995). ISBN 0-9522736-3-2.
5. A. Ernesti, J. M. Hutson and N. J. Wright (editors), "Fashioning a model: optimization methods in Chemical Physics" (1998). ISBN 0-9522736-4-0.

R. Prosmiti, J. Tennyson, D. C. Clary (eds.)
Molecular Quantum States at Dissociation

Microwave Spectroscopy of Ionic Complexes at the Dissociation Limit

A. Carrington, D.I. Gammie, J.C. Page and A.M. Shaw
Department of Chemistry, University of Southampton, Hampshire, SO17 1BJ, UK

The density of quantum levels near a dissociation limit is much greater than around the equilibrium geometry of a molecule and this has ramifications for the experimental investigation and theoretical description of the long-range interactions. This is particularly true for ionic complexes where the leading long-range interaction is the charge induced-dipole, which varies as r^{-4}, resulting in an interaction potential that supports vibration-rotation levels to very long range. In addition, the interaction of a spatially degenerate ionic state with an atom results in the formation of a number of electronic states which are degenerate at dissociation. The resultant small energy separations between the quantum states in this region of the potential enables microwave and millimetre wave radiation to probe not just conventional rotational transitions but also rovibronic transitions.

We have studied a number of ionic complexes [1] in this region of the potential using ion beam techniques and microwave spectroscopy. The experiment contains a number of important features that make it uniquely sensitive to the levels of interest. A diagram of the apparatus is shown in Fig. 1. The ions are produced in the source region of the apparatus and accelerated into an ion beam. Following mass selection the ions enter a copper waveguide where they interact with microwave radiation. The ion beam then passes through an electric field lens. All ions are unstable in an electric field and for the field strengths available in our laboratory (up to 40 kVcm^{-1}), only the levels within a few cm^{-1} of the dissociation limit fragment on a timescale necessary for detection. The fragments are then energy analysed to separate them from ions formed by spontaneous predissociation processes and are detected as a standing current on the off-axis multiplier at the end of the apparatus. When the frequency of the microwave photon is resonant with a transition in the molecule, the resulting population change is detected as either an increase or decrease in the fragment ion current if one or both levels dissociate in the electric field.

A further major experimental consideration is the production of ions in a beam that are populated in the levels near dissociation. Three methods have been employed: direct electron impact ionisation in the case of H_2^+, D_2^+, HD^+ and H_3^+ [2]; associative ionisation following electron impact excitation of He atoms, used in the investigations of the rare gas ion systems He_2^+ [3], $HeAr^+$ [4], $HeKr^+$ [5] and HeH_2^+ [6]; and finally electron impact ionisation of neutral clusters formed in a molecular beam, used in the investigations of Ar_2^+ and Ne_2^+ [7]. The latter technique required considerable modification to the source region of the apparatus whilst preserving the geometry of the ion optics. Vertical ionisation of the neutral species produced in the molecular beam exploits the difference in the equilibrium bond length between the weakly bound Van der Waals clusters and the much shorter equilibrium bond length of the ions. This results in the preferential population of the levels near the dissociation limit of the ion. In general, this also has the effect of preserving the rotational temperature of the neutral. However, the molecular beam can contain higher clusters, especially true of Ar_n, and fragmentation of these clusters produces Ar_2^+ ions which are more rotationally excited.

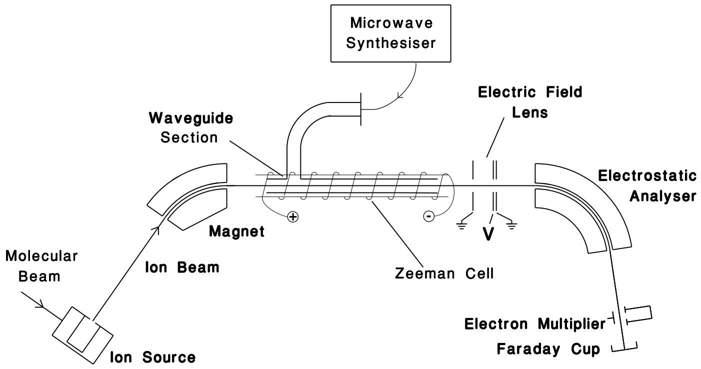

FIG. 1. Schematic diagram of the apparatus

Our first investigation of levels near the dissociation limit was in the hydrogenic species H_2^+, HD^+ and D_2^+. The excited electronic $2p\sigma_u$ state is essentially repulsive but at long range it has a shallow minimum. Unique *ab initio* calculations [8] of considerable accuracy predicted the microwave electronic spectrum, leading directly to its observation and assignment of the transitions. For these one-electron systems the agreement between experiment and theory was almost perfect. However, for the majority of molecules the *ab initio* calculations are inadequate for the level of accuracy required to predict the microwave electronic spectrum. Consequently the initial search, through the available frequency range (6–170 GHz) for a selection of different electric field strengths, is an unaided blind scan. Similarly, once a transition has been observed there is no assistance for the assignment. We have therefore employed the Zeeman effect and double resonance experiments to establish connectivities and J assignments for the

transitions. The Zeeman effect enables us to determine the J value and g-factor for both levels involved in the transition. The g-factor for each level then acts as a label for that level and transitions involving levels with identical g-factors can then be identified. We can use double resonance experiments to establish the common levels and construct a completely experimental pattern of the energy levels near to a dissociation limit.

The density of the energy levels near to the dissociation limit also complicates the theoretical description of the molecule. The spacing of all energy levels is comparable to the rotational constant of the molecule and enables terms in the rotational Hamiltonian to mix different states in a chosen basis set. The choice of the best quantum number basis set is not clear for the levels of interest and may change as the value of J increases. So for systems such as $HeAr^+$, the long-range interaction is $He(^1S)$ + $Ar^+(^2P_{3/2})$ and the initial choice of quantum numbers reflects the angular momentum coupling in the Ar^+ ion. The spin-orbit interaction in the ion is sufficient to couple $\boldsymbol{L}$ and $\boldsymbol{S}$ together to form the resultant $\boldsymbol{J_a}$, which on the approach of the He atom can have a projection quantum number Ω on the internuclear axis, forming a Hund's case (c) basis. Within this basis we are able to calculate the limiting g-factors for levels and can compare them directly with the observed values. For low J levels this is a good basis set. However, the rotational Hamiltonian contains terms that will mix the different $\Omega = 3/2$ and $1/2$ states and so Ω no longer remains a good quantum number. This is an example of rotational-electronic coupling and is a breakdown of the Born-Oppenheimer approximation.

In the case of $HeKr^+$ Hund's case (c) was a poor basis set for all J levels and case (e) was appropriate. Here the angular momentum of the ion, $\boldsymbol{J_a}$, couples directly to the mechanical rotational motion of the complex, $\boldsymbol{R}$, to form the resultant $\boldsymbol{J}$. This case was observed for the first time in the levels of $HeKr^+$. The difficulties with the choice of basis set makes an effective Hamiltonian analysis for these levels difficult and unreliable. To treat correctly all of the off-diagonal interactions the number of fitting parameters becomes large with respect to the amount of data and the fit is poorly determined. From an effective Hamiltonian analysis in $HeAr^+$ it is clear, however, that a full coupled channel calculation is required and this has been performed with the help of the BOUND program [9]. From the calculation of the energy levels using the close coupled channel technique we have been successful in deriving the complete interaction potential over the full range of internuclear separations for the rare gas systems $HeAr^+$, $HeKr^+$ and this is also nearing completion for Ne_2^+.

Having determined the interaction potential, it is possible to calculate the wavefunctions for the levels concerned and to calculate properties. The complete analysis produces g-factors in excellent agreement with those observed but also enables a calculation for the expectation values of bond lengths for the levels of the long-range ionic complexes. For $HeAr^+$ we were able to observe a level within 7 MHz of the dissociation limit that had a bond length of 15Å. This demonstrates the sensitivity of the technique to levels very close to dissociation of these truly long-range ionic complexes. For the $HeAr^+$ ionic complex, knowledge of the interaction potential at long range also enables transport properties of Ar^+ ions in He to be calculated making the important link between thermal collision dynamics and spectroscopy of the long-range states.

Investigation of the energy levels near a dissociation limit has enabled us to determine the entire interaction potential for the diatomic systems studied and has also stimulated considerable interest in the *ab initio* calculations of surfaces for these molecules. Extension of our investigations to larger clusters is a clear objective and we have made some observations of the microwave spectrum of HeH_2^+ [6]. The additional degrees of freedom in this molecule and an appropriate choice of quantum numbers has again proven difficult for this important ion-molecule prototype reaction. Beyond the triatomic systems are the larger Ar_n^+ ionic clusters which would provide interesting targets for spectroscopic and theoretical investigation.

[1] A. Carrington, A.M. Shaw and S.M. Taylor, J. Chem. Soc. Farad. Trans. **91**, 3725 (1995).
[2] (a) A. Carrington, C.A. Leach, R.E. Moss, T.C. Steimle, M.R. Viant and Y.D. West, J. Chem. Soc. Farad. Trans. **89**, 603 (1993); (b) A.Carrington, I.R. McNab, C.A. Montgomerie and R.A. Kennedy, Phys. Rev. Lett. **61**, 1573 (1988); (c) A. Carrington, I.R. McNab and C.A. Montgomerie, Chem. Phys. Lett. **160**, 237 (1989); (d) A. Carrington and R.A. Kennedy, J. Chem. Phys. **81**, 91 (1984); (e) A. Carrington, I.R. McNab and Y.D. West, J. Chem. Phys. **98**, 1073 (1993).
[3] A. Carrington, C.H. Pyne and P.J. Knowles, J. Chem. Phys. **102**, 5979 (1995).
[4] A. Carrington, C.A. Leach, A.J. Marr, A.M. Shaw, M.R. Viant, J.M. Hutson and M.M. Law, J. Chem. Phys. **102**, 2379 (1995).
[5] A. Carrington, C.H. Pyne, A.M. Shaw, S.M. Taylor, J.M. Hutson and M.M. Law, J. Chem. Phys. **105**, 8602 (1996).
[6] A. Carrington, D.I. Gammie, A.M. Shaw, S.M. Taylor and J.M. Hutson, Chem. Phys. Lett. **260**, 395 (1996).
[7] A. Carrington, A.M. Shaw and S.M. Taylor, Chem. Phys. Lett. **241**, 611 (1995).
[8] (a) R.E. Moss, Mol. Phys. **80**, 1541 (1993); (b) R.E. Moss, J. Chem. Soc. Farad. Trans. **89**, 3851 (1993).
[9] J.M. Hutson, BOUND computer program, version 5 (1993), distributed by Collaborative Computational Project No. 6 of the U.K. Engineering and Physical Sciences Research Council.

R. Prosmiti, J. Tennyson, D. C. Clary (eds.)
Molecular Quantum States at Dissociation

Long-Range Interactions Involving Atomic and Molecular Ions

Jeremy M. Hutson, Mark M. Law* and Markus Meuwly
Department of Chemistry, University of Durham, South Road, Durham, DH1 3LE, UK

I. INTRODUCTION

The long-range interactions between atoms and simple ions are of great importance in understanding solvation processes, in determining ion mobilities and capture cross sections and in processes such as Penning ionisation. However, high-quality experimental information on such interactions has been hard to come by.

Over the last few years, Alan Carrington's group at Southampton has developed novel ion beam methods for measuring the microwave spectra of ions in highly excited vibrational states, very close to dissociation. The methods depend on the fact that ionic states within a few cm^{-1} of the dissociation limit can be dissociated by an electric field. The population of such states can thus be monitored very sensitively by mass spectrometric detection of the fragmentation products.

Carrington and coworkers have observed near-dissociation spectra of species such as $He–Ar^+$, $He–Kr^+$, Ne_2^+, Ar_2^+ and $He–H_2^+$. The energy levels that exist so near to dissociation are quite novel in character, and there are no obvious patterns in the spectra: assigning quantum numbers to the lines is very difficult. Fortunately, there are some special features of the experiment that provide extra information beyond simple line frequencies:

- For many lines it is possible to observe Zeeman splittings, and in favourable cases this provides a direct measurement of the total angular momenta of the levels involved.
- Double resonance effects can sometimes be observed, and when they are they demonstrate that two lines share a common level.
- Sums or differences of two pairs of frequencies may be found to be the same; because of the very high resolution involved, such "quads" usually indicate that the two pairs represent transitions between the same two initial and final states, via different intermediate states.

*Present and permanent address: Department of Chemistry, University of Aberdeen, Meston Walk, Old Aberdeen, AB24 3UE, UK.

II. He–Ar$^+$ AND He–Kr$^+$

For He–Ar$^+$ [1], the near-dissociation spectra were sufficient to provide a partial energy level diagram. However, calculations were needed to establish the pattern of levels to be expected and to provide a full assignment. It was clear from the beginning that the interaction potential for He–Ar$^+$ was weak enough that the atomic L, S and J_a quantum numbers would be approximately conserved in the complex. Our initial expectation was therefore that the complex would follow Hund's case (c), in which the atomic J_a is quantised along the internuclear axis with projection Ω. This proved to be qualitatively correct, but the deviations from Hund's case (c) were too large for an "effective Hamiltonian" treatment based on it to be satisfactory [1]. Instead, it was necessary to carry out full coupled-channel bound-state calculations involving the three electronic states correlating with Ar$^+$ in its $^2P_{1/2}$ and $^2P_{3/2}$ states. Such calculations include all off-diagonal couplings directly, and thus implicitly incorporate Born-Oppenheimer breakdown. The interaction potential was initially quite poorly known, but it was possible to adjust it manually to reproduce the "assigned" part of the spectrum. The calculations then made it possible to understand the Zeeman g-factors and to assign additional lines that did not fit into the initial "experimental" energy level pattern.

This procedure was iterated several times: the spectra were used in a least-squares fit to refine the parameters of the interaction potential, and predictions based on the potential were then used to search for new lines. In many cases, new assignments could be tested because they predicted new quads or double-resonance relationships.

At the end of this process, we had observed and assigned 68 lines of He–Ar$^+$ corresponding to transitions between 37 levels lying within 8 cm^{-1} of dissociation. The levels and observed transitions are shown in Fig. 1. A remarkable feature of the spectra is that there appear to be no strong selection rules other than those arising from total angular momentum or parity. If case (c) coupling held, pure rotational transitions would be much stronger than vibrational or electronic transitions. However, in He–Ar$^+$ the breakdown of case (c) coupling is strong enough that transitions of all three kinds are seen with reasonable intensity.

The observed frequencies and g-factors have been fitted, together with limited information on lower levels from earlier ultraviolet spectra [2], to produce an interaction potential designated MAL1[1] for Ar$^+$ interacting with He [1]. Care was taken to ensure that the potential behaves correctly

[1]The functional form used is designated MAL, for Morse + anisotropic long range. MAL1 identifies this functional form and a particular set of optimised parameters.

at long range, where it has r^{-4} and r^{-6} contributions. The r^{-6} term is anisotropic, with different C_6 coefficients for the different electronic states involved: the spectra allowed this anisotropy to be identified and determined for the first time. The MAL1 potential has subsequently been used very successfully to interpret the mobilities of Ar$^+$ ions in He [3], which have been measured down to very low temperatures [4].

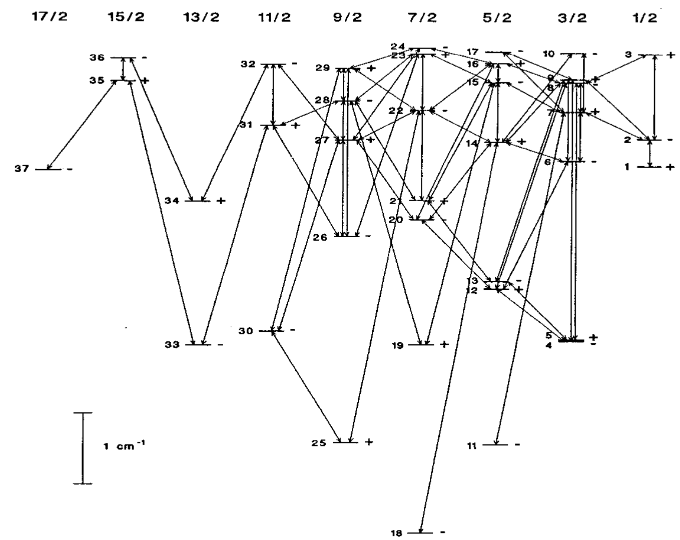

FIG. 1. Experimentally determined energy level diagram for He $\cdots$ Ar$^+$, arranged according to their J values and parity labels; the observed transitions are also shown.

The least-squares fits were carried out using the I-NoLLS program [5]. I-NoLLS is an interactive least-squares fitting package that allows the user to guide the progress of a least-squares fit through a highly-correlated parameter space, applying physical insight to select between different proposed steps in parameter space.

Carrington *et al.* have also observed near-dissociation spectra of He–Kr$^+$ [6]. We initially expected this to be similar to He–Ar$^+$. However the He–Kr$^+$ spectra were much sparser, with many fewer double resonances and "quads". The observed Zeeman effects also made much less sense than for He–Ar$^+$. Initial coupled-channel calculations on He–Kr$^+$ did not help much, as they simply suggested that the level pattern should be qualitatively similar to that for He–Ar$^+$. However, we eventually realised that the pattern could be explained if there was an accidental degeneracy between the vibrational levels supported (in a case (c) description) by the curves for the $|\Omega| = \frac{1}{2}$ and $\frac{3}{2}$ states. Under these circumstances, the resulting rovibronic states are complete mixtures of the $|\Omega| = \frac{1}{2}$ and $\frac{3}{2}$ states, and are best described by case (e) quantum numbers. In case (e), the Ω quantum number is destroyed, and instead the levels are characterised by a purely mechanical rotational quantum number R, which couples with J_a to form the total angular momentum J. None of the angular momenta have well-defined projections along the internuclear axis in case (e). The energy level pattern observed for He–Kr$^+$ is shown in Fig. 2.

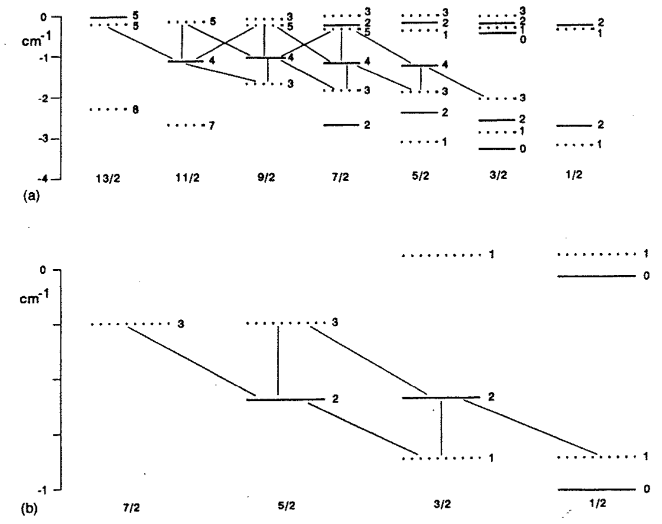

FIG. 2. (a) Energy level diagram close to the first dissociation limit, showing observed transitions. The energy levels are arranged in columns according to the values of J, and each level is also labelled with the value of R. Levels of positive parity are shown by dashed lines and negative parity by solid lines. The observed transitions involve a case (e) rotational manifold corresponding to v=4 for X state and v=3 for A_1 state. (b) Corresponding energy level diagram close to the second dissociation limit. The observed transitions are within the v=4 vibrational level.

Case (e) has quite different Zeeman effects from case (c). In particular, because case (e) has near-degeneracies between levels of the same R but different J, and these levels are coupled by the magnetic field, a first-order description of the Zeeman effects can be misleading. Because of this, some of the initial J assignments based on Zeeman splittings proved to be incorrect. However, all the Zeeman splittings could be rationalised on the basis of the coupled-channel calculations. In addition, case (e) has its own set of selection rules, based on $\Delta J = \pm 1$ and $\Delta R = \pm 1$. These are found

to be quite strictly followed in He–Kr$^+$, and this is why its spectrum is so much sparser than that for He–Ar$^+$.

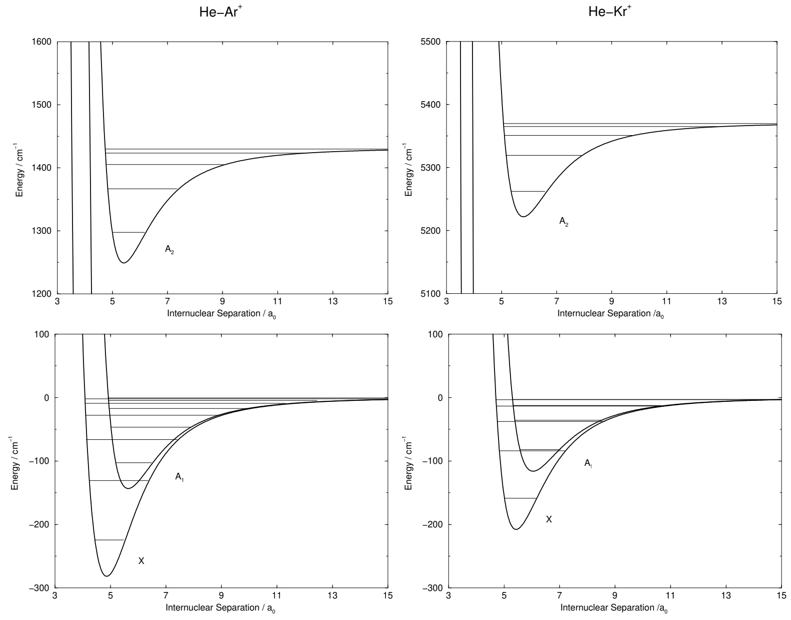

FIG. 3. Comparison of potential energy curves and vibrational energy levels for the three lowest electronic states of (a) He $\cdots$ Ar$^+$, A_2 state; (b) He $\cdots$ Ar$^+$, X and A_1 states; (c) He$\cdots$Kr$^+$, A_2 state; (d) He $\cdots$ Kr$^+$, X and A_1 states.

As for He–Ar$^+$, once an initial assignment had been obtained, it was possible to refine the potential parameters and search for additional lines. In this way, a complete energy level diagram was built up and an accurate interaction potential was obtained [6]. It is interesting and perhaps surprising to note that the well depth was determined to within 2% despite the fact that all the levels observed lie within 4 cm^{-1} of dissociation.

The MAL1 potentials for He–Ar$^+$ and He–Kr$^+$ are compared in Fig. 3. It may be seen that the levels supported by the $|\Omega| = \frac{1}{2}$ and $\frac{3}{2}$ states interleave one another for He–Ar$^+$, but that for He–Kr$^+$ there is a systematic near-degeneracy between the $|\Omega| = \frac{1}{2}$ level for vibrational quantum number v and the $|\Omega| = \frac{3}{2}$ level for vibrational quantum number $v' = v - 1$. The near-degeneracy first occurs for $v = 1$, $v' = 0$, but occurs systematically (and actually becomes closer) at higher v.

III. He–H_2^+

A few microwave lines involving near-dissociation states of He–H_2^+ have also been observed [7]. He–H_2^+ is a particularly interesting system, both from an astronomical point of view and because of extensive interest in $He^* + H_2$ Penning ionisation. The attractive well is sufficiently shallow that the near-dissociation bound states are regular, not chaotic as may be the case in species such as H_3^+. Carrington *et al.* have so far observed ten microwave lines of He–H_2^+, three of them with extensive hyperfine structure and others with intriguing Zeeman effects.

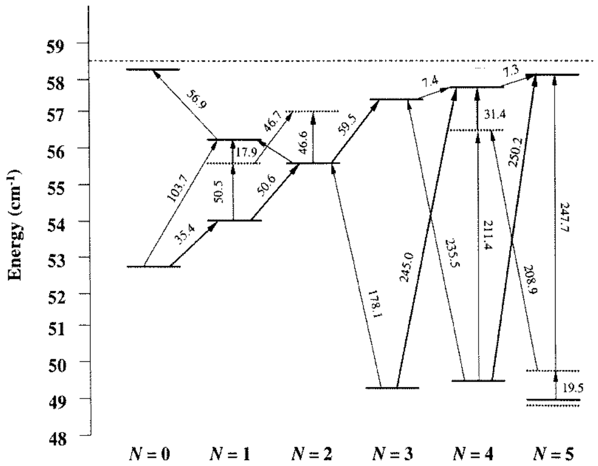

FIG. 4. See text for description.

Preliminary coupled-channel calculations of the near-dissociation levels [7], based on a two-dimensional potential energy surface by Falcetta and Siska [8], showed that near-dissociation levels of an appropriate type exist, but the potential surface was not good enough to provide an assignment. We have therefore carried out much more extensive calculations [9], using high-level *ab initio* methods, to obtain a new three-dimensional potential. The calculations were done with the quadratic CI (QCISD(T)) method, using Dunning's correlation-consistent aug-cc-pVQZ basis set. The calculations were carried out for 3 values of the H-H distance r on an extensive grid of values of the intermolecular distance R and angle θ. The points were then fitted to a 3-dimensional functional form, and used for

bound-state calculations. The resulting pattern of near-dissociation levels is shown in Fig. 4. The uppermost states generally have wavefunctions that peak at intermolecular distances between 10 and 12 a_0. The transition between a pair of $\mathcal{R}$-doublet levels for $N = 4$, $|\mathcal{R}| = 1$ is an attractive candidate for the best-studied of the microwave lines, which appears as a hyperfine multiplet near 15.2 GHz [7]. However, a considerable amount more work is needed to arrive at an unambiguous assignment and to understand the rest of the observed spectrum.

[1] A. Carrington, C. A. Leach, A. J. Marr, A. M. Shaw, M. R. Viant, J. M. Hutson and M. M. Law, "Microwave spectroscopy and interaction potential of the long-range He–Ar^+ ion", J. Chem. Phys. **102**, 2379 (1995).
[2] I. Dabrowski, G. Herzberg and K. Yoshino, J. Mol. Spectrosc. **89**, 491 (1981).
[3] L. A. Viehland and J. J. Hurly, J. Chem. Phys. **105**, 11143 (1996).
[4] N. Saito, T. M. Kojima, N. Kobayashi and Y. Kaneko, J. Chem. Phys. **100**, 5726 (1994).
[5] M. M. Law and J. M. Hutson, "I-NoLLS: a program for interactive nonlinear least-squares fitting of the parameters of physical models", Comp. Phys. Commun. **102**, 252 (1997).
[6] A. Carrington, C. H. Pyne, A. M. Shaw, S. M. Taylor, J. M. Hutson and M. M. Law, "Microwave spectroscopy and interaction potential of the long-range He–Kr^+ ion: an example of Hund's case (e)", J. Chem. Phys. **105**, 8602 (1996).
[7] A. Carrington, D. I. Gammie, A. M. Shaw, S. M. Taylor and J. M. Hutson, "Observation of a microwave spectrum of the long-range He–H_2^+ complex", Chem. Phys. Lett. **260**, 395 (1996).
[8] M. F. Falcetta and P. E. Siska, "The long-range interaction between He and H_2^+: an *ab initio* and dynamical study", Mol. Phys. **88**, 647 (1996).
[9] M. Meuwly and J, M. Hutson, "The potential energy surface and near-dissociation states of He–H_2^+", J. Chem. Phys. submitted (1998).

R. Prosmiti, J. Tennyson, D. C. Clary (eds.)
Molecular Quantum States at Dissociation

Quantum States of Triatomic Molecules at Dissociation

Rita Prosmiti, Hamse Y. Mussa and Jonathan Tennyson
Department Physics & Astronomy, University College London,
Gower Street, London WC1E 6BT, UK

I. INTRODUCTION

The calculation of the vibration-rotation spectrum of molecules up to their dissociation limit, and above, from potential energy surfaces is a long term problem and of central importance in chemical physics.

Traditionally, spectra of molecules have been analysed using a perturbative normal mode approach. For molecules where anharmonicity and intermode coupling are important, the traditional approaches fail to reproduce spectral patterns. This is particularly true in the dissociation region as the assumption of small amplitude vibrational motion, upon which most perturbative approaches are based, clearly fails. In general, to calculate energy levels accurately and to test or refine potential energy surfaces reliably, one must calculate eigenvalues of a matrix representation of the Hamiltonian operator. While such calculations are simple to formulate they are difficult to perform because, in most representations, it is necessary to construct and diagonalise very large scalar matrices to converge the energy levels. For this reason we have been exploring the use of novel computer architectures as a solution to this problem.

II. PDVR3D

Methods for treating the vibrational and rotational motion of triatomics based on the Discrete Variable Representation (DVR) have proved highly successful for spectroscopic studies [1]. However calculations on strongly bound systems up to and beyond dissociation can become computationally prohibitive [2]. For this reason we have re-written the triatomic DVR programs DVR3D [3] to run on computers with Massively Parallel Processors (MPP) such as the Cray-T3D and Cray-T3E at Edinburgh Parallel Computer Centre (EPCC) and the Cray-T3E at CINECA in Bologna.

The parallel version of DVR3D is known as PDVR3D. A full discussion of the algorithmic changes required to get PDVR3D to run efficiently have been given elsewhere [4,5]. For vibration only calculations, the program spreads the grid points of the final coordinate treated across the processors. As with conventional computers, the rate-limiting step of the calculation

remains the diagonalisation of the final matrix. We have successfully diagonalised dense, real-symmetric matrices of dimension up to 26976.

Rotational excitation is treated using the two step procedure of Tennyson and Sutcliffe [6]. To reduce I/O on the MPP system, it is found to be much more efficient to compute the matrix elements required for the second step of the calculation as part of the first step [5].

III. CALCULATIONS ON H_2O

Calculations have been performed for water up to dissociation using radau coordinates and two potential energy surfaces; that due to Varandas [7] which is parameterised using experimental data, and that due to Ho *et al.* [8] based on *ab initio* calculations. Calculations of the vibrational energy levels for this system find that both potentials support just over one thousand truly bound vibrational ($J = 0$) states. For example the potential of Ho *et al.* supports 587 even parity states and 489 odd parity ones. Such a calculation takes only about 20 minutes wall clock time using 64 processors on the EPCC Cray-T3E machine.

Calculations on rotationally excited states of water have also been performed. $J = 2$ levels for water have been obtained up to dissociation and studies of higher states of rotational excitation performed. Because these calculations are based on an appropriate Hamiltonian [9], the second step of the calculation is rapidly convergent. This means that for studies we have performed so far, CPU usage is dominated by the first step of the calculation, which scales as $(J+1)$ times the time taken for the $J = 0$ calculation, rather than the second step of the calculation which will scale as $(J+1)^2$ or $(J+1)^3$, depending on the number of levels required and the diagonaliser used.

Full details of these studies will be reported elsewhere [10]. Further calculations at this level should probably be coupled with the development of more reliable potential energy functions for water near its dissociation limit.

IV. CALCULATIONS ON H_3^+

Reliable nuclear motion calculations require a reliable underlying potential energy surface. As the first step towards studying H_3^+ at dissociation, we have constructed [11] an accurate global potential for the H_3^+ system. The energy switching approach was used to combine different functional forms for three different regions. The spectroscopically determined, Born-Oppenheimer surface of Dinelli *et al.* [12] was used for energies up to 20000 cm^{-1}; for higher energies the many-body expansion of Sorbie and Murrell [13] was fitted to *ab initio* calculations [14]; at large separations long-range terms were combined with accurate diatomic potentials. This approach produced an accurate global potential which represents all aspects of ground state H_3^+ including the avoided crossing of the two surfaces and dissociation limits. This surface is suitable for studying spectroscopy, high-lying bound states and reaction dynamics.

At present we are performing full 3D quantum calculations [15], for both zero and non-zero total angular momentum, using the above surface. We wish to pursue our attempts to understand Carrington *et al.*'s photodissociation spectra of H_3^+ [16]. The spectrum comprises transitions between the high lying vibrational states of the rotating molecule near the dissociation limit. Despite immense theoretical interest in this problem over the last decade, these spectra remain poorly understood and completely without even the crudest assignment of any feature.

Calculations on Carrington *et al.*'s spectrum are known to be very challenging [2] due to the high density of states, the floppiness of H_3^+, the strong coriolis interactions and the low barrier to linearity, which lead to various numerical difficulties. Furthermore, a true analysis of the spectrum will require consideration of quasi-bound states and their lifetimes.

Our potential, unlike those used for all previous studies in the dissociation region, correctly represents the attractive long-range interactions between H_2 and H^+. This leads to extra, extended vibrational states with consequent difficulty in performing reliable calculations.

We are performing our calculations for H_3^+ using PDVR3D. A DVR-direct product basis is used in Jacobi coordinates (θ,r,R). In this representation, particular attention should be paid to the choice of the grid along the R coordinate due to the singularity at $R = 0$, which corresponds to linear configurations. In the present work, a basis set of 96 sinc-DVR functions is used for the R coordinate to cover the whole R range up to dissociation. This basis is found [17] to be much more efficient than those used previously [18]. A further problem [18] arises from the failure of the quadrature approximation as $R \to 0$. Matrix elements of this type over sinc-DVR functions have been evaluated numerically which avoids shifts of energy levels and convergence problems. A final Hamiltonian of dimension nearly 25000 was diagonalised to calculate bound states up to dissociation with a convergence of 0.5 cm^{-1}. This calculation used a total of 12 hours to compute both even and odd symmetries on 96 Cray–T3E processors at EPCC. Of these, 11 hours were spent diagonalising the final Hamiltonian using the PARPACK iterative diagonaliser, requiring 700 eigenvalues for each symmetry.

For rotational states with $J \neq 0$, calculations are being performed using the DVR adaptation of the two-step method [19]. A previous, first attempt [2] to model Carrington *et al.*'s spectrum only included rotational states up to $J = 2$, known to be far too low; these calculations, took up to two weeks on a conventional computer. To model these spectra we need to study rotational states up to at least $J = 10$ and probably higher. These calculations are expensive; the required CPU time requirement will probably increase linearly with J. Calculations of this magnitude clearly represent a computational grand challenge.

V. DISCUSSION

Calculations using PDVR3D have been performed on a number of triatomics. In particular ozone, HCP and most recently on the astronomically important N_2H^+ molecular ion, for which vibrational levels were obtained up to dissociation [20].

Advances in computer technology and methodology allow us to study more challenging problems. However, the H_3^+ case shows that further improvements are necessary if we want to tackle important problems at the dissociation limit and beyond.

ACKNOWLEDGMENTS

This work was performed as part of the EPSRC ChemReact High Performance Computing Initiative (HPCI) Consortium. R.P. gratefully acknowledges a TMR Fellowship under contract ERBFMBICT 960901 and ICARUS 2 project (CINECA) under EC contract ERBFMGECT 950052.

[1] Z. Bačić and J.C. Light, “Theoretical methods for rovibrational states of floppy molecules”, Ann. Rev. Phys. Chem. **40** 469 (1989).

[2] J. R. Henderson and J. Tennyson, “Calculated spectrum for near-dissociation H_3^+: a first attempt”, Mol. Phys. **89**, 953 (1996).

[3] J. Tennyson, J.R. Henderson and N.G. Fulton “DVR3D: programs for fully pointwise calculation of ro-vibrational spectra of triatomic molecules”, Comp. Phys. Comms. **86**, 175 (1995).

[4] H.Y. Mussa, J. Tennyson, C.J. Noble and R.J. Allan, “Rotation-vibration calculations using massively parallel computers”, Comp. Phys. Comm. **108**, 29 (1998).

[5] H.Y. Mussa, J. Tennyson, C.J. Noble, and R.J. Allan, “Molecular rotation-vibration calculations using massively parallel computers”, in *High Performance Computing*, R.J. Allan, A.D. Simpson and D.A. Nicole (eds.), (Plenum, 1998).

[6] J. Tennyson and B.T. Sutcliffe, “A generalised approach to the calculation of ro-vibrational spectra of triatomic molecules”, Mol. Phys. **58**, 1067 (1986).

[7] A.J.C. Varandas, “Energy switching approach to potential surfaces: An accurate single-valued function for the water molecule”, J. Chem. Phys. **105**, 3524 (1996).

[8] T.-S. Ho, T. Hollebec, H. Rabitz, L.B. Harding and G. Schatz, “A global H_2O potential energy surface for the reaction $O(^1D) + H_2 \to OH + H$”, J. Chem. Phys. **105**, 10472 (1996).

[9] J. Tennyson and B.T. Sutcliffe, "Discretisation to avoid singularities in vibration-rotation Hamiltonians: a bisector embedding for AB_2 triatomics", Intern. J. Quantum Chem. **42**, 941 (1992).
[10] H.Y. Mussa and J. Tennyson, "Calculation of the rotation-vibration states of water up to dissociation", J. Chem. Phys. submitted, (1998).
[11] R. Prosmiti, O.L. Polyansky and J. Tennyson , "A global potential energy surface for the H_3^+ molecule", Chem. Phys. Lett. **273**, 107 (1997).
[12] B.M. Dinelli, O.L. Polyansky and J. Tennyson, "Spectroscopically determined Born-Oppenheimer and adiabatic surfaces for H_3^+, H_2D^+, D_2H^+ and D_3^+", J. Chem. Phys. **103**, 10433 (1995).
[13] J.N. Murrell, S. Carter, S.C. Farantos, P. Huxley and A.J.C. Varandas, *"Molecular Potential Energy Functions"*, (Wiley, New York, 1984).
[14] R. Schinke, M. Dupuis and W.A. Lester, Jr., "Proton - H_2 scattering on an *ab initio* CI potential energy surface. Vibrational excitation at 10 eV", J. Chem. Phys. **72**, 3909 (1980).
[15] R. Prosmiti, M.Y. Mussa, O.L. Polyansky and J. Tennyson, "Quantum states of H_3^+ at dissociation", in preparation.
[16] A. Carrington, I.R. McNab and Y.D. West , "Infrared predissociation spectrum of the H_3^+ ion", J. Chem. Phys. **98**, 1073 (1993).
[17] V.A. Mandelshtam and H.S. Taylor, "The quantum resonance spectrum of the H_3^+ molecular ion for J=0. An accurate calculation using filter diagonalization", J. Chem. Soc., Farad. Trans. **93**, 847 (1997).
[18] J. R. Henderson, J. Tennyson and B.T. Sutcliffe, "All the bound vibrational states of H_3^+: a reappraisal", J. Chem. Phys. **98**, 7191 (1993).
[19] J. Tennyson, "Rotational excitation with pointwise vibrational wavefunctions", J. Chem. Phys. **98**, 9658 (1993).
[20] H.Y. Mussa, S. Schmatz, M. Mladenovic and J. Tennyson, "Bound vibration-rotation states of N_2H^+ up to dissociation", J. Chem. Phys. to be submitted, (1998).

R. Prosmiti, J. Tennyson, D. C. Clary (eds.)
Molecular Quantum States at Dissociation

Highly Excited Rotational Dynamics of H_3^+

I. N. Kozin and R. M. Roberts
Mathematics Institute, University of Warwick, Coventry CV4 7AL, UK

I. INTRODUCTION

Considerable interest has been shown in highly rotationally excited states of molecules. This has been motivated by new theoretical and experimental investigations of the predissociation spectrum of H_3^+ [1], critical phenomena in water-like molecules [2,3], variational calculations of CF_4 [4,5] and the dissociation and rearrangements of argon clusters [6,7], to name just a few. In each of these areas an analysis of the classical system has proved to be very useful since it provides physical insights into the rotational dynamics of the molecular system, something which is usually lacking in variational calculations of molecular spectra. The classical and quantum approaches to the same molecule should therefore be viewed as complementary.

The results described here have been developed from earlier works by Zhilinskii, Pavlichenkov and Kozin [2,8] and Roberts, Sousa Dias and Montaldi [9] on *relative equilibria* of molecules. These are classical trajectories corresponding to steady rotations of molecules about stationary axes during which the shapes of the molecules remain constant. The main idea is to take advantage of the fact that the total angular momentum $\boldsymbol{J}$ is an integral of motion and the Hamiltonian can be regarded as being parameterised by $J = |\boldsymbol{J}|$. This approach resembles in many respects the works of Lohr on argon clusters [7]. It also lies behind the general formalism of Jellinek and Li [10] describing the separation of rotational energy and in particular their analysis of $\boldsymbol{J}$-dependent normal vibrational modes. Related concepts appear in the work of Miller and Wales [11], who classify relative equilibria (there called stationary points) by their Hessian indices, and in the analysis of angular momentum barriers to dissociation in multi-atomic molecules by Pollak [12] and Chambers and Child [13]. A unifying theme of all these methods is their use of the so-called effective potential function $V_{\text{eff}} = V(\boldsymbol{q}) + 1/2\,\boldsymbol{J}\boldsymbol{I}^{-1}\boldsymbol{J}$ which incorporates both the potential and rotational energy and drives the molecular dynamics in the vicinity of the relative equilibria.

The present work gives a detailed description of *all* relative equilibria of the H_3^+ ion and how they change as the total angular momentum increases, assuming an isolated ground electronic state. We are aware of the fact that at high energies the influence of other electronic states must be taken into account [14] and our analysis at energies close to dissociation should only be considered as giving a rough idea of what might happen. It is a major problem to extend the classical analysis given here to two-fold potential energy surfaces or to points of energy surface switching. However we were surprised to find that the global maps of relative equilibria of H_3^+ as functions of J are qualitatively similar for a model pairwise potential based on just one Morse function and for the recent very accurate potential due to Dinelli, Polyansky and Tennyson [15]. All the results below are given for this latter potential. Full details will appear in [16].

II. THE PROCEDURE

An appropriate Hamiltonian for non-linear configurations of a molecule is given in [8] and for dynamics near a linear reference configuration in [16]. In both cases the Hamiltonian looks like

$$H = \frac{1}{2}\boldsymbol{J}\boldsymbol{\mu}\boldsymbol{J} - \boldsymbol{J}\boldsymbol{C}\boldsymbol{p} + \frac{1}{2}\boldsymbol{p}\boldsymbol{B}\boldsymbol{p} + V \tag{1}$$

where $\boldsymbol{q}$ is an appropriate vector describing the shape of the molecule, $\boldsymbol{p}$ is the corresponding vector of momenta, $\boldsymbol{\mu}$ is an inverted modified inertia tensor, $\boldsymbol{C}$ is a matrix describing the Coriolis interaction, $\boldsymbol{B}$ is the vibrational kinetic energy matrix, and V is the potential energy function. The matrices $\boldsymbol{\mu}$, $\boldsymbol{C}$ and $\boldsymbol{B}$ and the function V all depend on $\boldsymbol{q}$. For triatomic molecules the vectors $\boldsymbol{q}$ and $\boldsymbol{p}$ are three dimensional for the non-linear Hamiltonian and four dimensional for the linear Hamiltonian. In the latter case an extra symmetry and conserved constraint are used to recover the correct dimension.

The equations of motion are straightforward for coordinates and momenta:

$$\dot{q}_n = \partial H/\partial p_n \ ; \ \ \dot{p}_n = -\partial H/\partial q_n \tag{2}$$

while the equations for the angular momentum $\boldsymbol{J}$ make use of Poisson brackets:

$$\dot{J}_\alpha = \{J_\alpha, H\}. \tag{3}$$

The relative equilibria are the points in phase space where all time derivatives are zero. For fixed $\boldsymbol{J}$ the equilibrium solutions of Eqs. (2) are precisely the solutions of $\partial V_{\text{eff}}/\partial q_n = 0$, i.e. the stationary points of the effective potential. For the particular case of triatomic molecules, setting the right hand side of Eq. (3) to zero shows that the direction of $\boldsymbol{J}$ must be either in, or perpendicular to, the molecular plane. This set of equations for the relative equilibria can be obtained in an analytic form and then

solved numerically using MATHEMATICA and the total energies of the relative equilibria plotted as functions of J. An example is given in Fig. 1.

The next step is to consider small oscillations around each of the relative equilibria. The normal modes and their frequencies are found by diagonalising the linearised equations of motion. In general the frequencies are distinct and the normal modes are mixtures of the internal 'shape oscillations' and precessional motion. If all the frequencies are real the relative equilibrium is said to be linearly stable and the classical phase space nearby is dominated by bound trajectories. If the relative equilibrium is a minimum of the Hamiltonian, and so its Hessian matrix has no negative eigenvalues, then it is automatically linearly stable. However it is important to note that a relative equilibrium may also be linearly stable if its Hessian matrix has any even number of negative eigenvalues. An example is provided by the maximum energy relative equilibrium of an asymmetric rotor.

III. RESULTS

A classical picture of the rotational dynamics of the H_3^+ ion and its isotopic modifications up to and above the dissociation limit has been obtained by a global study of their relative equilibria and stabilities. Several remarkable phenomena were observed. For example H_2D^+ exhibits critical phenomena similar to those predicted for water [2] and observed in H_2Se [3]. However, unlike for water-type molecules, the equilibrium bending angle is less than 90° and there is not only a bifurcation of the in-plane stable precession axis but also of the in-plane unstable axis.

It was confirmed that for H_3^+, H_2D^+ and D_2H^+ the lowest energy relative equilibrium has linear geometry at sufficiently high values of the total angular momentum J [12,13]. Furthermore the series of bifurcations and changes of stability that accompany the transfer of stability from the rotating equilateral triangle configuration (in the H_3^+ case) to a linear configuration have been computed (see Fig. 1 for H_3^+).

Interestingly, the rotating equilateral triangle remains linearly stable for a large range of angular momentum values beyond the point where it ceases to be a minimum of the energy function. In this range, the Hessian matrix of the Hamiltonian has two negative eigenvalues but the frequencies remain real. In a quantum model this should correspond to a mode with an energy pattern which decreases in energy rather than increasing as for lower values of the angular momentum.

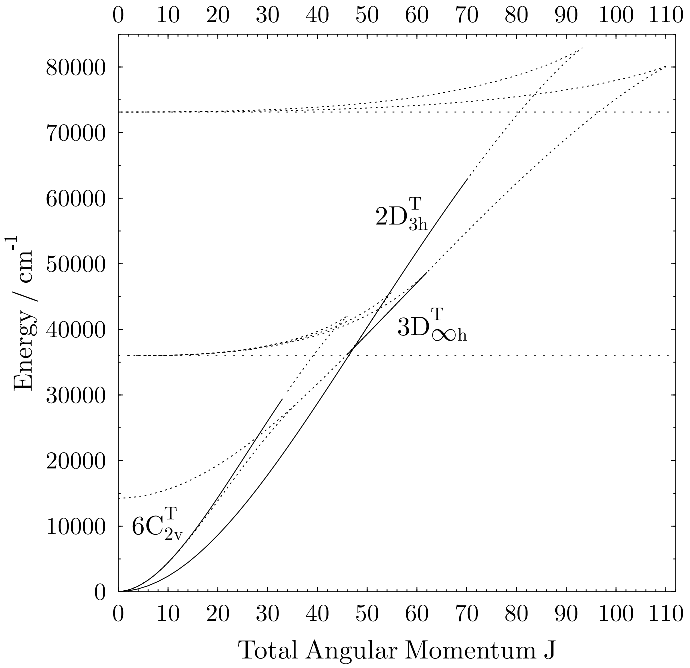

FIG. 1. The energies of linearly stable (solid lines) and unstable (dotted lines) relative equilibria of the H_3^+ ion are shown as functions of the total angular momentum J. The symmetry groups of the stable relative equilibria are indicated together with the degeneracy. The T-superscript in the symmetry group notation denotes that these groups include time reversal symmetries. They are isomorphic to the corresponding point groups. The two horizontal dotted lines indicate the dissociation energies of the ion.

The fate of linearly stable relative equilibria with negative Hessian eigenvalues is usually a Hamiltonian Hopf bifurcation, i.e. as J increases the frequencies of two normal modes become equal and then complex, the normal modes simultaneously becoming unstable [17]. This happens not only to the rotating equilateral triangle relative equilibria of H_3^+, but also to the relative equilibria corresponding to the maximum rotational energy of the J-multiplets, and to their analogues for H_2D^+ and D_2H^+.

Ultimately all relative equilibria collide with matching rotational barriers to dissociation at sufficiently high J. However before this happens there is a considerable region of phase space containing bound classical trajectories, even above the dissociation limit. We hope that these will correspond to

interesting patterns in the quantum spectrum.

ACKNOWLEDGMENTS

We are grateful to Jonathan Tennyson and Boris Zhilinskii for a number of very useful discussions. This work is supported by an EPSRC research grant.

---

[1] A. Carrington and R. Kennedy, J. Chem. Phys. **81**, 91 (1984).
[2] B.I. Zhilinskii and I.M. Pavlichenkov, Opt. Spectrosc. (USSR) **64**, 413 (1988).
[3] I.N. Kozin, S.P. Belov, O.L. Polyansky and M.Yu. Tretyakov, J. Mol. Spec. **152**, 13 (1992).
[4] S. Brodersen, J. Mol. Spec. **145**, 331 (1991).
[5] B.I. Zhilinskii, S. Brodersen and M. Madsen, J. Mol. Spec. **160**, 192 (1993).
[6] D.H. Li and J. Jellinek, Z. Phys. D. **12**, 177 (1989).
[7] L.L. Lohr and C.H. Huben, J. Chem. Phys. **99**, 6369 (1993); L.L. Lohr, Mol. Phys. **91** 1097 (1997).
[8] I.N. Kozin and I.M. Pavlichenkov, J. Chem. Phys. **104**, 4105 (1996).
[9] R.M. Roberts and M.E.R. de Sousa Dias, Nonlinearity **10**, 1719 (1997); J.A. Montaldi and R.M. Roberts, to appear in J. Nonlin. Sci. (1998).
[10] J. Jellinek and D.H. Li, Phys. Rev. Lett. **62**, 241 (1989); Chem. Phys. Lett. **169**, 380 (1990).
[11] M.A. Miller and D.J. Wales, Mol. Phys. **89**, 533 (1996).
[12] E. Pollak, J. Chem. Phys. **86**, 1645 (1987).
[13] A.V. Chambers and M.S. Child, Mol. Phys. **65**, 1337 (1988).
[14] R. Prosmiti, O.L. Polyansky and J. Tennyson, Chem. Phys. Let. **273**, 107 (1997).
[15] B.M. Dinelli, O.L. Polyansky and J. Tennyson, J. Chem. Phys. **103**, 10433 (1995).
[16] I.N. Kozin, R.M. Roberts and J. Tennyson, in preparation.
[17] J.C. van der Meer, *Lecture Notes in Mathematics* **1160**, (Springer-Verlag, Berlin, 1985).

R. Prosmiti, J. Tennyson, D. C. Clary (eds.)
Molecular Quantum States at Dissociation

Signal Processing as a Computational Tool for Chemical Dynamics

Howard S. Taylor
Department of Chemistry, University of Southern California,
Los Angeles, CA 90089-0482, USA

The signal processing method (SPM) of computation has brought a new view point to the field of chemical calculations. The method [1,2] has shown itself capable of enabling the efficient calculation of highly excited and densely packed bound states, resonances and of reactive cross sections in energy ranges near dissociation. Reference [1] is the key paper with all the details of this computational methodology as used by this author and his co-workers, in particular V. Mandelshtam. Reference [1] contains the references that space limits forbids repeating here.

The SPM method has two basic parts, signal generation (SG) and signal processing (SP). The SG part, which involves the heavy calculation characteristic of chemical dynamics, produces at equally spaced quasitimes n ($t = n\tau$; τ is a fixed measurement interval yielding a bandwidth of $2\pi/\tau$; $n = 1 \ldots N$; $N\tau = \max t$) a generically complex signal $C_n^{\beta\alpha}$ which is assumed to be of the form of a correlation function, i.e. $C_n^{\beta\alpha} = (\Phi_\beta \exp[-i\Omega n]\Phi_\alpha)$. This will be the required input for SP. Here Φ_α and Φ_β are initial and final packets respectively, that characterise the problem of interest e.g. channel state packets or packets in the full interaction region which can be propagated in quasitime with the purpose of extracting poles, i.e. bound states and/or resonances. Ω is the operator controlling the dynamics. For our purposes Ω is the Hamiltonian operator H, or a function of H which contains the ever essential potential surface. A matrix notation can be introduced to handle multiple surface problems. Once the SG produces a sufficiently long sequence of $C_n^{\beta\alpha}$, then the SP part of the problem extracts the residues and poles that are all that is needed to determine the Green's function of Ω (or H) evaluated between Φ_α and Φ_β. The poles on the negative real axis are bound state energies, the poles lying near the real axis in the fourth quadrant of the complex energy plane give the energy and lifetime (width) of the resonances and the collection of all poles and residues determine the Green's function between Φ_α and Φ_β and hence the $S_{\beta\alpha}$ matrix element. The extraction procedure, i.e. the signal processing procedure, is that first introduced by Wall and Neuhauser [2] and reformulated for efficiency, simplicity and ultimately useability by Mandelshtam and Taylor [1]. We outline the SG and SP parts of our methodology and compare it to more standard approaches so as to reveal the advantages and disadvantages the new method presents.

Any propagation method that constructs $\exp[-i\Omega t]\Phi_\alpha$ can generate the $C_n^{\beta\alpha}$ for input into the SP. Many methods, ours included, start with a sparse matrix representation of H and essentially generate the sequence Φ_α, $\mathrm{H}\Phi_\alpha$, $\mathrm{H}^2\Phi_\alpha \ldots$. This matrix multiplication of H on a vector, since the basis or grid is large, is the computationally time consuming step. Picking a basis or grid of size M on which the H matrix is sparse, reduces the effort to an $M \ln M$ scaling by allowing the programs to concentrate on the "small" number of non-zero elements in the matrix multiplication and not on multiplying by a zero that a straight matrix-vector multiplication would entail. For the computations of bound states resonances and scattering poles we choose Φ_α to have random amplitudes at the DVR grid points that serves as our basis. The DVR assures sparsity. The randomness assures that with care, the initial state has amplitude on any eventually extracted eigenstate. Now the H on a vector program is used to drive the three term Chebyshev recursion relation to produce the Chebyshev polynomial (in H) vector $T_n(\mathrm{H})\Phi_\alpha$ [$\mathrm{H}^n\Phi_\alpha$ is needed for T_n] which is then used to simply produce, for any α ($\beta = \alpha$ for bound states and resonances) the desired $C_n^{\beta\alpha}$ by recognising that $T_n(\mathrm{H}) = \cos(\mathrm{n}\Omega) = \mathrm{Re}\exp[-\mathrm{i}\Omega\mathrm{n}], \Omega = \cos\mathrm{H}$. For bound states the standard Chebyshev recursion relation is used. For continuum problems we have introduced a modified Chebyshev recursion relation. For both cases Ref. [1] gives variants of this procedure that are optimally efficient for the SG as well as the SP. The modified Chebyshev is exactly as the usual Chebyshev except that T_{n+1} and T_{n-1} are replaced by $e^{+\gamma}T_{n+1}$ and $e^{-\gamma}T_{n-1}$ in the recursion in which T_n^γ and T_{n-1}^γ give T_{n+1}^γ. Here $i\gamma$ is the usual negative imaginary absorbing potential placed in the channels at their point of contact with the interaction region. The use of γ greatly diminishes matrix size by eliminating the requirement of having grids that go down the channel. Alternately it can be viewed as damping wavepackets (here it damps the T_n polynomials) in the channels so that unphysical, interference causing, reflections from the ends of the grid, do not occur. As $\gamma \to 0$ the usual Chebyshev results. Both T_n and T_n^γ in their respective domains, can be used to construct Greens functions for H and $\mathrm{H} + i\gamma$ respectively or to construct $\Psi(t) = \exp[-i\mathrm{H}t]\ \Phi_\alpha$ for the bound and continuum case. Most methods that generate Chebyshev polynomials do this latter construction; we do not! We only produce the $C_n^{\beta\alpha}$, ($\alpha = \beta$ for bound states) for use in the SP process. In dynamical problems our method retains the "all energies in one propagation" property.

The above procedure has some nice properties. First storage is modest, only three vectors need be stored at one time. Second, real as opposed to complex numbers and operations only are used in the computationally heavy parts of the problem, thereby increasing efficiency by a factor of four. Importantly the Chebyshev series is globally (all energy) and uniformally convergent and numerically stable. In particular round off error is not a problem in the SG or SP part of our methodology. As such when we signal process to get eigenvalues we can expect, and have so far noted, no multiple eigenvectors; a problem which occurs in the Lanczos method of diagonalisation which also requires the same $\mathrm{H}^n\Phi_\alpha$, $n = 1 \dots M$ to diagonalise. Multiple eigenvectors are a problem solved in Lanczos by using extra iterations. This is an advantage but before we celebrate, we note that the SP process we use to get the eigenvalues will require a number of $C_n^{\beta\alpha}$ greater than M for its own but different reason as discussed below. In fact the present method requires a substantial number of iterations to converge the bound states or resonances but a pay off in numerical stability and global convergence as well as an ability to resolve, after signal processing, closely spaced interior eigenvalues will be the resulting strong point. Lanczos only efficiently resolves closely spaced eigenvalues at the ends of the spectrum. A great deal of extra work is needed for Lanczos to obtain such interior eigenvalues.

Prior to our introduction of the damped Chebyshev polynomial much less efficient Chebyshev based methods were used to propagate packets to obtain $\Psi(t)$ and to eventually create correlation functions. These methods as all such methods, were forced to use the absorbing potential and this led to the expansion of $\exp[i\mathrm{H}t]$ in the T_n to diverge after a small number of n's. This problem was solved by repeatedly stopping the computation after a short time propagation, damping the packet and restarting again. This latter method is clearly less efficient. If Chebyshev iterations were our only problem we can expect convergence of propagators and eigenvalues to require a number of iterations proportional to $2\rho\ \Delta\mathrm{H}$, where ρ is the density of states or spectral peaks and $\Delta\mathrm{H}$ is the energy range of the spectrum. As ρ gets large near dissociation the need for heavy computation emerges in both Lanczos and Chebyshev methods. Since ρ is determined by the system under study, nothing can be done about it. A search for basis sets that retains sparseness and reduces $\Delta\mathrm{H}$ might be worth while if we had any good ideas on this, which we don't. Our view is that we can accept the price of more iterations easier than numerical instabilities and the non-resolution of interior eigenvalues.

Now we turn to the SP part of the problem. For contrast we note that even though we have the ability now to create a $\Psi(t)$ we shall not do this as then to get eigenvalues, we would have to create the correlation function $(\Psi(0)\Psi(t))$ and either subject it to a discreet Fourier transform (FFT) or evaluate it at $t = n\tau$ to use the SP method. We do not do the former as the $C_n^{\beta\alpha}$ based on the Chebyshev are, as stated, already acceptable correlation

functions at quasitimes n and the only price we pay to use them is that the output eigenvalue is the cosine of the energy eigenvalue; a problem easily remedied. We do not do the latter because in general a much shorter signal length, N, is needed to obtain poles from our signal processing procedure than from FFT. The FFT, to resolve, needs an N inverse to the minimum real energy spacing between adjacent poles. Our signal processor (denote it SPFD for Filter Diagonalisation) will need N proportional to the inverse of the average spacing; a much smaller N for all but harmonic oscillators. This is also a big work saver in any problem that employs packet propagation be it semi-classical or quantum. SPFD needs to propagate for shorter N, i.e. shorter quasitime. Moreover since the FFT produces a spectrum first and fits it to Lorentzians to get pole parameters (i.e. energies and widths) it cannot separate overlapping resonances. The SPFD method obtains poles first and then constructs spectra and can untangle "overlaps" which do not appear as such in the complex energy plane.

Now to the SPFD itself. First note that it does not matter to SPFD how the signal $C_n^{\beta\alpha}$ was created; they can even be of experimental origin. As such the α, β superscripts can be dropped and C_n can replace it. The method assumes the signal results from a dynamics involving some Ω, Φ_α, and Φ_β which it need not know and which characterises for the user the physical system. In fact it will produce the generically complex frequencies (energies) and residues (their spectral strength; both magnitude and phase) by diagonalising a matrix whose matrix elements are known in terms of the available C_n. When the C_n are assumed to be of the correlation matrix element form given above, it is easy to demonstrate [1,2] that, if formally the complex symmetric [Hermitian if real eigenvalues or stick spectra only occur] operator Ω (or better $\exp[i\Omega]$) is diagonalised, that the eigenvalues yield the generically complex frequencies ω_k that delineate the position of the pole in the complex angular frequency plane. Furthermore if the formal closure of eigenfunctions (χ_k) is inserted into the C_n matrix element to allow its spectral evaluation, the signal C_n, will be consistent with a form which is the sum of K weighted damped harmonics or exponentials, $d_k \exp[-i\omega_k n]$. Here d_k and ω_k are complex and d_k is formally $(\Phi_\alpha, \chi_k)^2$; again a point similar to Lanczos. Hence the SPFD can be viewed as a way to achieve a non-linear fit of the N C_n to an harmonic form with K pairs of complex parameters(d_k, ω_k) ; hence the name "Harmonic Inversion" that SP methods of this type are given in the engineering literature. Amazingly this can be done by solving a linear eigenvalue problem associated with the operator $\exp[-i\Omega]$. Algebra says that to achieve the fit N must be $N \geq 2K$. Since K is the number of angular frequency eigenvalues over the spectral angular range 2π it is roughly $2\pi/\Delta\omega_k$ (average). This yields the convergence or resolution criteria mentioned above, $N \geq 4\pi/\Delta\omega_k$

(average). The spectrum, obtained formally by the Fourier transform of the correlation function fit is therefore modelled by a sum of Lorentzians each of which is the residue weight d_k divided by $(\omega - \omega_k)$. The better the model, and it certainly is good for resonances, the smaller will be N and the more stable will be the results to changing N and internal computational parameters.

The reason that we need never specify Ω and Φ_α is that if the operator $\exp(-i\Omega)$ is represented on a orthogonal Krylov basis set, $\Phi_n = (\exp[-i\Omega])^n \Phi_\alpha, n = 1, 2, ... \approx N/2$, a generalised matrix linear eigenvalue problem emerges in which the n, m element of the operator and overlap matrix is the given C_{n+m+1} and C_{n+m} respectively. Note we do not need Ω as its matrix representation is known! The matrices are called data matrices and are a conventional starting point of such standard signal processing schemes as Linear Predictor and Auto Regressive methods (ARMA). In fact we could, using the above information, quickly derive these methods if we make the added assumption that we know K, the number of Lorentzians needed to fit the spectrum. K which is often the number of spectral lines or resonances, is usually completely unknown and must be obtained by finding a region of K values where the spectrum is invariant to change in K. The situation is actually at this point quite bad as the above matrices are quite ill-conditioned in that the rank is smaller than the dimension i.e. $N/2$ and worse they are large as N is large. In such cases not only is computing time excessive but instability and round-off error occurs even when methods as singular value decomposition (SVD) are used. These often yield incorrect and spurious roots. It is often possible to detect which roots are spurious by observing their instability to repeated calculation in which N, basis size and the power of the operator to be diagonalised are changed. But this is impractical when the computation time is long and the number of roots is large. It is at this point that Neuhauser made his main contribution to signal processing by suggesting that the Filter diagonalisation (FD) method be used to diagonalise the matrix of the operator $\exp[-i\Omega]$. FD will break the big matrix up into an array of partly overlapping much smaller diagonal blocks such that diagonalisation could be achieved block by block or spectral window by spectral window. Here, as the matrices are small, SVD is less troublesome (ill conditioning is still present) computing time is much less and the search for stable roots is easier since repeated diagonalisations with changing N, operator power etc. is not costly. Neuhauser chose as his filter a Gaussian. This turned out to be inefficient and introduced unnecessary parameters that needed to be varied for optimisation. Mandelshtam and Taylor used a box filter which introduced no new parameters and made the method more efficient and transparent without sacrificing the advantages of the

rapid computation of the spectrum in a window followed by a repeat of the procedure for all desired spectral window regions. The whole procedure is in effect a linear transform type of change of basis from the Krylov basis Φ_n, to a new basis Ψ_j. Ψ_j is taken as a linear combination of M basis functions Φ_n with coefficients $\exp[in\phi_j]$. Here the ϕ_j are angular frequency grid points on the unit circle in the complex angular frequency plane. The Fourier nature of this transformation coefficient suggest that $\Delta n \Delta \phi_j \approx 2\pi$. This ϕ_j means that the basis Ψ_j is, if n gets high enough,a packet localised around ϕ_j and as such windowing is due to the fact that matrix elements between such packets are small when such packets are far from each other. In fact the elements die off with their index difference x as $\sin x/x$. Since the matrix elements in the Krylov basis is known in terms of the C_n and the basis transformation coefficients are known, the matrix elements in the new basis are known in terms of the points ϕ_j and the C_n. In actuality the sum involved here is the most time consuming step but it scales roughly as $N \ln N$ making our timing similar to the FFT (storage requirements are also similar). The introduction of windowing achieves two extra important aims. Relative to LP methods the dependence of results on K is gone, as it is meaningless in a theory that calculates windows of eigenvalues from small matrices that are independent of each other. Similarly the interior-exterior eigenvalue problem disappears for similar reasons. A window matrix is too small (order 10^2 x 10^2 to have such an eigenvalue distinctions and the windows do not know if they are at the ends or inside the bigger matrices. A disadvantage has also been here introduced. Since n needs to achieve a "high" value to localise Ψ_j and to then window, more C_n may be needed. This and the $N \geq 4\pi/\Delta\omega_{av}$ is where in the diagonalisation problem based on Chebyshev iterations, the number of needed iterations (for $T_n\Phi_\alpha$ and therefore $C_n^{\alpha\beta}$) increased beyond what the Lanczos might need.

In rough summary the procedure for obtaining the poles ω_k and the residues d_k obtained using the eigencoefficients resulting from the small matrix diagonalisation and the matrix elements of our exponential operator in the angularly localised basis is as follows. First one picks a window which one expects to have a modest number of eigenvalues. Then one picks a grid of J ϕ_j that is evenly spaced over the window and of size greater than the expected number of eigenvalues. Even a poorly converged FFT can sometimes be useful to estimate the number of expected eigenvalues. Reducing window size allows dimensions, i.e. J, to be kept less than about 100. Then one uses the N C_n and J ϕ_j points to construct the matrix elements and applies SVD to the generalised eigenvalue problem. The problem is repeated for slight changes N to test convergence and for root stability by changing N (on a smaller scale) and/or J and/or the power of the operator used. Unstable roots are rejected as spurious or as numerical or experimental noise (we assume most noise is poorly represented by Lorentizians and sensitive to parameters). Once the poles, ω_k and residues d_k are obtained the bound eigenvalues or resonant energies and lifetimes are known; spectra can be evaluated and S matrices can be evaluated. The different dynamical problems are specified by the choice of the Φ_α and Φ_β. For experimental signals the fact that we have obtained the signal peak frequency, width, weight and phase allows the more revealing type absorption spectra to be constructed along with the ability to use shorter signals and to reduce noise.

As an example we shall present for the NO_2 molecule a computation of all its bound vibrational eigenvalues using the lowest two intersecting and interacting potential surfaces [3]. This is a most challenging problem.

---

[1] H.S. Taylor and V.A. Mandelshtam, "Harmonic inversion of time signals and its applications", J. Chem. Phys. **107**, 6756 (1997).

[2] M.R. Wall and D. Neuhauser, "Extraction, through filter-diagonalization, of general quantum eigenvalues or classical normal mode frequencies from a small number of residues or a short-time segment of a signal. I. Theory and application to a quantum-dynamics model", J. Chem. Phys. **102**, 8011 (1995).

[3] R.F. Salzgeber, V. Mandelshtam, Ch. Schlier and H.S. Taylor, "All the adiabatic bound states of NO_2", J. Chem. Phys. **109**, 937 (1998).

R. Prosmiti, J. Tennyson, D. C. Clary (eds.)
Molecular Quantum States at Dissociation

Getting the Most out of Time Signals: From NMR to Quantum Dynamics Calculations.

V.A. Mandelshtam
Department of Chemistry, University of California, Irvine, CA 92697-2025, USA

We briefly review some very recent results associated with the filter diagonalisation method (FDM), which is a rapidly developing approach for the spectral analysis of time signals arising, in particular, in molecular dynamics calculations, including calculations of quantum spectra of molecular systems at dissociation.

The conventional strategy for analysing the spectrum of a time signal by using the Fourier transform (FT) wastes a lot of useful information contained in the signal, whether the latter has been measured in an experiment or calculated by, e.g., solving the time dependent Schrödinger equation. Even though the ideas of extracting maximum information from time signals in molecular dynamics calculations occurred independently, they are actually very reminiscent to those in the spectral analysis of Nuclear Magnetic Resonance (NMR) time signals. The need to obtain the "linelist" (the line positions, widths, amplitudes and phases) more than a decade ago led the NMR community to try to develop and implement, as alternative to FT, "high resolution" methods of spectral analysis (see, e.g., Ref. [1]), usually based on various linear algebraic techniques to solve the harmonic inversion problem

$$C(t) = \sum_k d_k e^{-itE_k} \tag{1}$$

for the unknown complex frequencies $E_k = \epsilon_k - i\Gamma$ and weights d_k. Surprisingly, none of those techniques worked well enough to be useful in practical applications. However, FDM, first invented by Wall and Neuhauser [2] and then improved significantly by us [3,4], turned out to be the method of choice, demonstrating unprecedented numerical performance. While here we are mostly interested in the spectral analysis of small quantum molecular systems, we note that FDM will undoubtedly become very common in NMR as well.

Several versions of FDM now exist. For example, the general FDM for solving Eq. (1), to extract the resonance parameters (linelist) from the decaying time [2,4] or Chebyshev [4] correlation functions. Once one decided to consider the "exact" quantum calculations involving propagation of a wave function, the time correlation functions, as, e.g.,

$C_{\alpha\alpha'}(t) = \langle\Phi_\alpha|\exp(-i\hat{H}t)\Phi_{\alpha'}\rangle$, become formally equivalent to the Chebyshev correlation functions, $c_{\alpha\alpha'}(n) = \langle\Phi_\alpha|T_n(\hat{H})\Phi_{\alpha'}\rangle$, as both can be fit to the form more of Eq. (1) [4]. However, for numerical implementations the latter are far superior as there is no need to exponentiate the Hamiltonian matrix and any numerical problems with correct implementation of the absorbing boundary conditions for a dissociative system are avoided [5]. Note though that the time-dependent formulation is more natural for implementing various kinds of approximations, e.g., classical or semiclassical (SC), in which case FDM is also very useful often leading to a significant reduction of the propagation time [6].

Although for bound state calculations one can use the general FDM, another version [3] is much more efficient as it implements effectively the constraint corresponding to a non-decaying, purely real, spectrum. The latter version is also based on the inversion of the Chebyshev correlation functions (see the corresponding applications in Refs. [3,7]).

When a time signal decays in time, due to physical relaxation processes, or gets corrupted, due to imperfections of the measurement or calculation (e.g., because of inadequate numerical accuracy for describing the dynamics of very closely spaced quantum energy levels [2], or very broad and therefore rapidly decaying resonances in a molecular system [8], or breakdown of the semiclassical approximation of time correlation functions [9], etc.), only a finite portion of such a signal carries useful information. This information might be far from adequate to describe the spectral properties of the system in question, even when very efficient methods of spectral analysis are used. The very purpose of multidimensional NMR is to increase the amount of information accumulated by the time signals for a finite and short time. This is achieved by considering multidimensional time signals (e.g., 2D spin echoes) with relatively short extensions of the signal in the auxiliary dimensions, each point in these dimensions corresponding to another experiment.

Just as in NMR, in molecular dynamics calculations one can increase the amount of information per time unit by propagating $L > 1$ initial wave packets and generating the $L \times L$ time cross-correlation matrix $C_{\alpha\alpha'}(t)$ to be inverted by solving

$$C_{\alpha\alpha'}(t) = \sum_k b_{\alpha k} b_{\alpha' k} e^{-itE_k} \quad (2)$$

with the unknown complex frequencies E_k and amplitudes $b_{\alpha k}$. This idea was first mentioned in Ref. [2] in the context of resolving two degenerate or quasi-degenerate quantum energy levels using FDM, and then utilised in the calculation of complex resonance energies with very large widths, i.e., with very fast decay rates. In Refs. [9,10] it was demonstrated that a long time quantum dynamics can be described adequately by short

time cross-correlation matrices computed using SC approximations based on the initial value representation (IVR). The advantage of the SC IVR approximation is that calculations of the time correlation functions only require the propagation of classical trajectories, i.e. it allows us, at least in principle, to handle multi-dimensional systems. The disadvantage is that it is only correct for a short time. In other words, the classical trajectories do not do exactly what the quantum system is supposed to do, e.g., they do not tunnel through a barrier. Surprisingly, the use of the cross-correlation matrices overcomes this conceptual difficulty. The simple informational argument is that an $L \times L$ cross-correlation matrix carries by about a factor of L more information than a single , say, autocorrelation function. Hence for sufficiently large L we can reduce the propagation time below the breakdown limit, as in Ref. [9] to extract tunnelling splittings from a real time SC propagation. This same idea also worked well for the problem of periodic orbit quantisation [11]. Compared to the original implementation of the method using a single Gutzwiller periodic orbit sum [12], the use of the cross-correlated SC signal allowed the reduction of the number of periodic orbits by orders of magnitude.

In Ref. [10] we also showed that the time cross-correlation functions have other useful applications. For example, it is possible in the framework of the "exact" quantum approach to obtain a complete description of the dynamics of the system in terms of the transition matrix elements between various states (e.g., all the S-matrix elements) from a single wave packet propagation, a seemingly contradictory result according to the intuition developed in the conventional "time-dependent" approaches, where a column of the S-matrix is usually obtained at a time (see, e.g., Refs. [13,14]).

In conclusion we point out that the FDM for solving Eq. (1) seems to have become an essentially "black box" numerical algorithm, also being very stable with respect to various kinds of noise, while the extensions of FDM, such as those to invert Eq. (2), do not; the main reason being that the "noise" due to the approximate nature of the cross-correlation signal can easily destroy the assumed form of Eq. (2). This creates a challenge for both the problem of generating a "clean" SC signal and its efficient processing.

[1] D.S. Stephenson, Progress in NMR Spectroscopy, **20**, 515 (1988); J.C. Hoch and A.S. Stern, NMR Data Processing, (Wiley-Liss, New York, 1996).

[2] M.R. Wall and D. Neuhauser, "Extraction, through filter-diagonalization, of general

quantum eigenvalues or classical normal mode frequencies from a small number of residues or a short-time segment of a signal. I. Theory and application to a quantum-dynamics model", J. Chem. Phys. **102**, 8011 (1995).

[3] V. A. Mandelshtam, and H. S. Taylor, "A low-storage filter diagonalization method for quantum eigenenergy calculation or for spectral analysis of time signals", J. Chem. Phys. **106**, 5085 (1997).

[4] V. A. Mandelshtam, and H. S. Taylor, "Spectral analysis of time correlation function for a dissipative dynamical system using filter diagonalization. Application to calculation of unimolecular decay rates", Phys. Rev. Lett. **78**, 3274 (1997); V. A. Mandelshtam, and H. S. Taylor, "Harmonic inversion of time signals and its applications", J. Chem. Phys. **107**, 6756 (1997).

[5] V.A. Mandelshtam and H.S. Taylor, "The spectral projection approach to the quantum scattering calculations", J. Chem. Phys. **102**, 7390 (1995); "A simple recursion polynomial expansion of the Green's function with absorbing boundary conditions. Application to the reactive scattering", J. Chem. Phys. **103**, 2903 (1995); V.A. Mandelshtam, "Global recursion polynomial expansions of the Green's function and time evolution operator with absorbing boundary conditions", in *Multiparticle Quantum Scattering with Applications to Nuclear, Atomic and Molecular Physics*, IMA Volumes in Mathematics and its Applications, Eds.: Don Truhlar and Barry Simon, **89**, 389 (1996).

[6] F. Grossmann, V. A. Mandelshtam, H. S. Taylor, and J.S. Briggs, "Harmonic inversion of semiclassical short time signals", Chem. Phys. Lett. **279**, 355 (1997).

[7] R. F. Salzgeber, V. A. Mandelshtam, Ch. Schlier and H. S. Taylor, "All the adiabatic bound states of NO_2 ($J = 0$)", J. Chem. Phys. **109**, 937 (1998).

[8] E. Narevicius, D Neuhauser, H.J. Korsch and N. Moiseyev, "Resonances from short time complex-scaled cross-correlation probability amplitudes by the filter-diagonalization method", Chem. Phys. Lett. **276**, 250 (1997).

[9] V. A. Mandelshtam and M. Ovchinnikov, "Tunneling splittings from a real-time semiclassical propagation". J. Chem. Phys. **108**, 9206 (1998).

[10] V. A. Mandelshtam, "Harmonic inversion of time cross-correlation functions. The optimal way to perform quantum or semiclassical dynamics calculations", J. Chem. Phys. **108**, 9999 (1998).

[11] J. Main, K. Weibert, V. A. Mandelshtam, and G. Wunner, "Semiclassical spectra and diagonal matrix elements by harmonic inversion of cross-correlated periodic orbit sums", Phys. Rev. Lett. submitted, (1998).

[12] J. Main, V. A. Mandelshtam, and H. S. Taylor, "Periodic orbit quantization by harmonic inversion", Phys. Rev. Lett. **79**, 825 (1997).

[13] D.J. Tannor and D.E. Weeks, " Wave packet correlation function formulation of scattering theory: the quantum analog of classical S-matrix theory", J. Chem. Phys. **98**, 3884 (1993).

[14] D.J. Kouri, Y. Huang, W. Zhu, D.K. Hoffman, "Variational principles for the time-independent wave-packet-Schrödinger and wave-packet-Lippmann-Schwinger equations", J. Chem. Phys. **100**, 3662 (1994).

R. Prosmiti, J. Tennyson, D. C. Clary (eds.)
Molecular Quantum States at Dissociation

Dynamics and Statistics in the Unimolecular Dissociation of NO_2

S. Yu. Grebenshchikov, C. Beck, J. Hauschildt,
H. Flöthmann and R. Schinke

Max-Planck Institut für Strömungsforschung
Bunsenstraße 10, D-37073 Göttingen, Germany

Unimolecular dissociation — i.e., fragmentation of an isolated polyatomic molecule excited above the first dissociation threshold — is one of the fundamental chemical processes [1]. It has been intensively studied in the past and still is under thorough investigation today. For an indepth introduction we recommend two monographs, Refs. [2] and [3]; extensive list of references can be found in three recent reviews, Refs. [4–6]. The focal point of most experimental and theoretical investigations is the microcanonical dissociation rate constant $k(E)$ and its dependence on the energy of the system. In the present paper we concentrate almost exclusively on calculations of $k(E)$. There exists today a rich variety of different prescriptions for extracting the rate constants and for understanding the dissociation mechanisms [3]. Two main lines of attack can be distinguished. The *'statistical'* approach assumes a separable reaction coordinate and a uniform, time independent distribution of the internal energy over the available degrees of freedom. These assumptions enable one to express the rate constant $k(E^\dagger)$ through the sum of states at the transition state (TS), $N^\ddagger(E^\dagger)$, and the density of the reactant states, $\rho(E^\dagger)$,

$$k(E^\dagger) = \frac{N^\ddagger(E^\dagger)}{h\rho(E^\dagger)}\,, \tag{1}$$

where $E^\dagger$ is the energy in excess of the dissociation threshold D_0. The input information in Eq. (1) is restricted and, therefore, highly averaged over the internal states of the molecule. Depending on the definition of the TS and $N^\ddagger$ one distinguishes several theories: the famous RRKM theory, its variational version, phase space theory (PST), and the statistical adiabatic channel model (SACM) [3]. A statistical approach is quite natural for describing early experimental results, obtained for thermal systems with broad internal energy distributions and even for microcanonical ensembles in which the initial quantum state of parent molecules remains unspecified. A long list of successful applications of statistical theories can be found in Ref. [3].

However, present experimental techniques enable one to study dissociation on a *state-to-state* level, i.e., to follow the decay of a given initial quantum state into a particular quantum product channel [5]. New effects become observable in the reaction dynamics, such as fluctuations of rates, their mode — or state — specificity, signatures of the TS wave functions in the product state distributions etc. Prominent experimental studies include HCO [7], DCO [8,9], NO_2 [10], D_2CO [4], and CH_3O [11,12]. As a result, the features, which are intentionally averaged out in the statistical approach, can turn significant in understanding new experimental findings. This is where an alternative *'dynamical'* approach to unimolecular dissociation becomes essential. It consists in solving either the Newton (Hamilton) equations of motion (classical molecular dynamics) or the time–dependent or time–independent Schrödinger equation (quantum molecular dynamics). In principle, the applicability of the dynamical approach is independent of whether or not the statistical assumptions are fulfilled. Constant progress in computer hardware as well as recent advances in numerical algorithms for performing quantum calculations [13,14] enabled in the past few years quantum mechanical investigations of small-size systems on a unprecedented level of detail. Molecules which have been tackled so far are HCO [15], DCO [16], H_3^+ [17], HNO [18], HOCO [19]. It is an extremely demanding task to extend exact dynamical calculations to larger polyatomic molecules; both the accurate potential energy surfaces (PESs) and the schemes for dynamical (quantum) calculations are currently not available. In order to understand mechanisms of state-to-state dissociation one is bound to study small polyatomics, essentially triatomics. It is more than coincidence, however, that triatomics are also convenient objects for state–resolved experiments [5]. The initial and product states of the system can be clearly specified, and the relatively low density of states of the parent molecule warrants that the state–specific effects are not washed out during the experiment. A special group of small molecules is made up by those whose eigenstates are ergodic. For them, the statistical assumptions are expected to be applicable, and the results of dynamical and statistical calculations can be justly compared. As a result, one might gain insight into the question why the dissociation of so many molecules can be described in a statistical manner.

In what follows we discuss the dynamical (quantum and classical) and statistical dissociation rates for nitrogen dioxide, NO_2, the benchmark system which has been the focus of many systematic experimental and theoretical studies. Our goal is to see which features of the dissociation process are correctly grasped by the transition state theory (TST) (Eq. (1)). In order to provide a broader overview, it is necessary to make references to other molecules. We choose HCO and HNO for this purpose. They

were the subjects of a recent review Ref. [6]. One can anticipate some problems in the application of TST to NO_2, HNO, and HCO. On the one hand, the dynamics of highly vibrationally excited NO_2 is dominated by vibronic chaos [20], and the molecule is believed to decay in a purely statistical manner. This certainly favours the TST. At the same time, the reaction is barrierless, so that the position of the TS in the reaction is poorly defined. The same also applies to HNO. In HCO, there is a small barrier towards dissociation. However, the HCO molecule has a very regular bound spectrum, and its dissociation is strongly mode–specific.

The global three–dimensional PESs for these molecules were calculated *ab initio*. An important point is that both dynamical *and* statistical calculations are performed using the *ab initio* potentials.

Calculation of the quantum mechanical dissociation rates requires the concept of resonances [21]. Resonances are the poles of the Green's function of the system in the complex plane. One can think about them as eigenstates with the real energies E_n substituted by $E_n - i\Gamma_n/2$. This formula implies that the norm of the corresponding eigenfunction decays exponentially in time. This enables one to introduce a quantum dissociation rate by

$$k_n = \Gamma_n/\hbar\,. \tag{2}$$

The individual quantum rates for the NO_2 molecule were obtained by the solution of the time–dependent Schrödinger equation. Modified Chebyshev polynomials [17] were used to expand the time evolution operator. The calculated rates are plotted in Fig. 1 vs. the excess energy $E^\dagger$. The characteristic rate k_{ave}, defined as an average of the individual rates over a narrow energy window, grows slightly with increasing $E^\dagger$. k_{ave} correlates well with the experimental results of Wittig *et al.* [22]. At the same time, quantum rates demonstrate large fluctuations, the amplitude of which reaches two orders of magnitude. They are most pronounced in the first 300 cm^{-1} above D_0.

Of course, strongly fluctuating dissociation rates are the rule rather than exception for small molecules. In the HNO molecule, which is also close to being statistical, the fluctuation pattern is similar to that depicted in Fig. 1 [6].

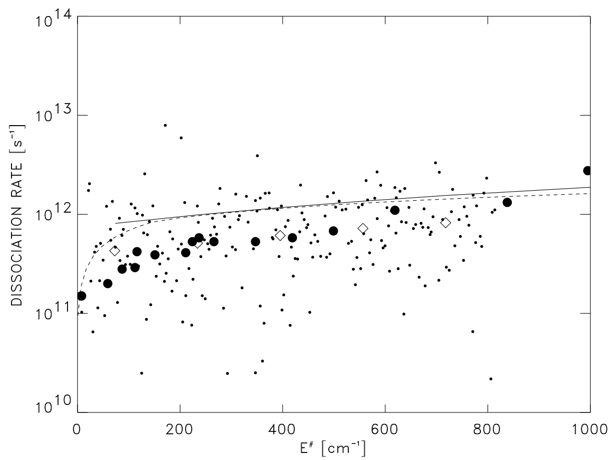

FIG. 1. Dissociation rates for NO_2 vs. the excess energy $E^\dagger$. Dots – quantum mechanical calculations; diamonds - slow rate in the classical trajectory calculations; solid line – RRKM rate; dashed line – SACM rate; solid circles – experimental results of Ref. [22].

Fluctuations have been measured, for example, for HCO [7], DCO [8,9], D_2CO [4], and CH_3O [12]. Fluctuation rates were also the subject of thorough theoretical investigations [23]. The analysis suggests, that *for a fully statistical system* the normalised dissociation rates k/k_{ave} are distributed according to a chi–squared distribution with N_{TS} degrees of freedom, where N_{TS} is the number of open channels at the TS. With increasing N_{TS} — which means with growing $E^\dagger$ — this distribution becomes narrower and develops a pronounced peak at $k/k_{\mathrm{ave}} \approx 1$. One expects strong fluctuations only in systems which are *not* statistical and it is quite surprising to see them in NO_2, the molecule famous for its chaotic dynamics, even 800 cm^{-1} above D_0. It is worth mentioning, however, that the scale of fluctuations is comparatively modest. In the regular HCO, the rates fluctuate over more than three orders of magnitude even 1.5 eV above the dissociation threshold (see Fig. 9 in Ref. [6]). Keeping this in mind, one may say that the rates in NO_2 show some correlation with the statistical prediction.

Deviations from the statistical decay can also be seen in the results of classical calculations. In order to obtain classical dissociation rates one constructs distributions, $P(t_{\mathrm{TS}})$, of trajectory lifetimes t_{TS}. The lifetime t_{TS} is the time of the first crossing of the TS. One example of such probability distribution for NO_2 is shown in Fig. 2.

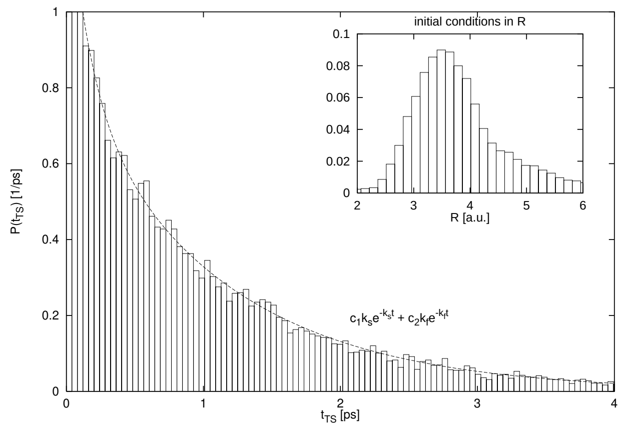

FIG. 2. Lifetime distribution function $P(t_{\mathrm{TS}})$ for NO_2. t_{TS} is the time at which the trajectory reaches the TS. Shown in the inset is the distribution of the trajectory initial conditions along the dissociation coordinate. The RRKM TS is located at 6 a_0.

If the dynamics of the dissociating molecule were completely irregular, the lifetimes would be random and $P(t_{\mathrm{TS}})$ would be an exponential function. This is certainly not the case for NO_2: one needs at least two exponentials to fit $P(t_{\mathrm{TS}})$. Very similar two–exponential lifetime distributions were also found for HNO and for regular HCO [6]. The reason for the existence of two rate constants, a fast one and a slow one, is that the phase space of the molecule is split into several parts which are weakly coupled on the dissociation time scale. In the NO_2 molecule, the main contribution to the fast decay rate comes always from the portion of the phase space immediately adjacent to the TS: trajectories with a significant initial excitation in the dissociation coordinate reach the TS very quickly and thus lead to a very large rate. More detailed considerations [24] show that these "fast" trajectories do not fulfill the statistical assumption: the time of energy redistribution in the system is larger than their lifetime! One may exclude these trajectories from the analysis and study only the slow classical rate. This rate is shown in Fig. 1 as function of energy. It demonstrates very reasonable agreement with the experimental data and goes right through the quantum mechanical points. The same behaviour of the slow classical rate was observed in HCO and HNO.

A natural question arises from the above analysis: how do the statistical models cope with the fact, that the molecular break–up is apparently non–statistical? Two statistical approaches were analysed, the variational RRKM and the SACM [3]. They employ the same Eq. (1) for the rate constant, but differ in the way in which the number of states at the TS are counted. The SACM counts the quantum states at the TS, while the variational RRKM counts the classical states. They both use, however, the same density of states $\rho(E^{\dagger})$. Since the total density of states above D_0 is divergent, one *extrapolates* the density of bound states to positive $E^{\dagger}$. One operates on the premise that the density of the reactive states is a continuation of the density of bound states. The statistical dissociation rates for NO_2 are shown in Fig. 1. The SACM and RRKM rates correlate well with each other. The statistical rates are also in surprisingly good agreement with the state–resolved quantum mechanical results, and with the classical mechanical and experimental rates. The statistical theories predict the rate constant, which is just a factor of two too high. The rate is overestimated because the statistical models assume the uniform population of the *whole* available phase space at $t = 0$. Remember, that according to the classical mechanical considerations, the phase space near the TS is not ergodic. It is worth to note, that for HNO and even for HCO the statistical rates are greater than the dynamical ones roughly by the same factor of two.

Two conclusions may be drawn from our discussion. First, the performance of the statistical models in estimating the dissociation rates is exceptional. If TST works for small triatomic molecules with low density of states, one can expect it to be even better for bigger molecules and potentials with deeper wells. Second, dynamical calculations are indispensable in describing the *actual* dissociation mechanism. Note that the agreement between the observed and statistical rates is not a sufficient condition for the reaction to be truly statistical. Dissociation of NO_2, HNO, and HCO are the best examples. The average rate constant is, in some sense, a very robust feature of the dissociation process. More details about state–specific rates are necessary in order to unravel the mechanism of unimolecular reactions. These details can be obtained only through dynamical calculations.

ACKNOWLEDGMENTS

R.S. and S.Yu.G. wish to thank Antoine Delon for many fruitful discussions on the dynamics of the NO_2 molecule. S.Yu.G. is grateful for financial support from the Alexander von Humboldt Stiftung.

[1] K. J. Laidler, *Theories of Chemical Reaction Rates.* (McGraw-Hill, New-York, 1969).
[2] R. G. Gilbert and S. C. Smith, *Theory of Unimolecular and Recombination Reactions.* (Blackwell, Oxford, 1990).

[3] T. Baer and W. L. Hase, *Unimolecular Reaction Dynamics.* (Oxford University Press, Oxford, 1996).
[4] W. H. Green, Jr., C. B. Moore and W. F. Polik, Annu. Rev. Phys. Chem. **43**, 591 (1992).
[5] S. A. Reid and H. Reisler, J. Phys. Chem. **100**, 474 (1996).
[6] R. Schinke, C. Beck and S. Grebenshchikov H.-M. Keller, Ber. Bunsenges. Phys. Chem. **102**, 593 (1998).
[7] J. D. Tobiason, J. R. Dunlop and E. A. Rohlfing, J. Chem. Phys. **103**, 1448 (1995).
[8] J. D. Tobiason, J. R. Dunlop and E. A. Rohlfing, Chem. Phys. Lett. **235**, 268 (1995).
[9] C. Stöck, X. Li, H.-M. Keller, R. Schinke and F. Temps, J. Chem. Phys. **106**, 5333 (1997).
[10] B. Abel, H. H. Hamann and V. Lange, Faraday Discuss. Chem. Soc. **102**, 147 (1995).
[11] A. Geers, J. Kappert, F. Temps and J. W. Wiebrecht, J. Chem. Phys. **99**, 2271 (1993).
[12] S. Dertinger, A. Geers, J. Kappert, F. Temps and J. Wiebrecht, Faraday Discuss. Chem. Soc. **102**, 31 (1995).
[13] R. E. Wyatt and J. Z. H. Zhang (Eds.), *Dynamics of Molecules and Chemical Reactions.* (Marcel Dekker, Inc., New York, 1996).
[14] J. Chem. Soc. Farad. Trans. **93** (1997). Special issue on quantum theory of chemical reactions.
[15] H.-M. Keller, H. Floethmann, A. J. Dobbyn, R. Schinke, H.-J. Werner, C. Bauer and P. Rosmus, J. Chem. Phys. **105**, 4983 (1996).
[16] H.-M. Keller, T. Schröder, M. Stumpf, C. Stöck, F. Temps, R. Schinke, H.-J. Werner, C. Bauer and P. Rosmus, J. Chem. Phys. **106**, 5359 (1997).
[17] V. A. Mandelshtam and H. S. Taylor, J. Chem. Soc. Farad. Trans. **93**, 847 (1997).
[18] C. Beck, S. Yu. Grebenshchikov, H.-M. Keller, H. Flöthmann, D. H. Mordaunt, A. J. Dobbyn and R. Schinke, J. Chem. Phys. in press (1998).
[19] E. M. Goldfield, S. K. Gray and G. S. Schatz, J. Chem. Phys. **102**, 8807 (1995).
[20] A. Delon, R. Georges and R. Jost, J. Chem. Phys. **103**, 7740 (1995).
[21] L. D. Landau and E. M. Lifshitz. *Quantum Mechanics. Nonrelativistic Theory.* (Pergamon, New York, 1976).
[22] S. I. Ionov, G. A. Bruckner, C. Jaques, Y. Chen and C. Wittig, J. Chem. Phys. **99**, 3420 (1993).
[23] U. Peskin, H. Reisler and W. H. Miller, J. Chem. Phys. **101**, 9672 (1994).
[24] S. Yu. Grebenshchikov, C. Beck, H. Flöthmann, R. Schinke and S. Kato, in preparation (1998).

R. Prosmiti, J. Tennyson, D. C. Clary (eds.)
Molecular Quantum States at Dissociation

Predissociation Dynamics of $HeBr_2$ near the $Br_2(B)$ Dissociation Limit

Marta I. Hernández, Tomás González–Lezana,
Gerardo Delgado–Barrio and Pablo Villarreal
Instituto de Matemáticas y Física Fundamental (C.S.I.C.)
Serrano 123, E-28006-Madrid, Spain

I. INTRODUCTION

The X-BC complexes (X= rare gas atom, BC=dihalogen molecule) have become prototypes for the study of molecular energy transfer and intermolecular forces of van der Waals (vdW) systems. The main process in these systems is vibrational predissociation (VP): an initial quasibound state X-BC(v_0) in a electronically excited state, decays to X + BC($v_f < v_0$) by energy transfer from the BC vibrational motion, labelled by v_0, to the vdW modes. Potential energy surfaces (PES) for these molecules can be tested in great detail since, assuming a given PES, accurate dynamical calculations can be performed and compared against detailed measurements (sometimes at a state-to-state level) of spectral shifts, VP rates and product distributions [1].

As experiments can be performed for a range of initial vibrational excitations, v_0, the rare gas-halogen interaction is probed as a function of the interhalogen separation, r. Obviously, more information on vdW forces is achieved if a sufficiently large range of v_0 levels is investigated. It seems particularly interesting to explore the transition from small r (low v_0's), where the the system may be regarded as a closed shell molecule weakly interacting with a rare gas atom, to the case where the average distance between the halogen atoms is so large that one should think of two open shell atoms interacting between them and with the rare gas atom. The predissociation dynamics near dissociation of the dihalogen subunit is possibly ruled by new mechanisms that are worth investigating.

$HeBr_2$ is perhaps the molecule for which the largest range of vibrational levels have been studied in some detail: v_0 = 8–48 (note that the average Br-Br separation varies from 2.8 Å to a value as large as 5.5 Å for the above v_0-range). van de Burgt *et al.* [2] first recorded laser induced fluorescence spectra for v_0 = 11–38. A higher range of vibrational levels ($v_0 = 34$–48) was studied by Jahn *et al.* [3] using the pump-probe spectroscopic technique. Surprisingly, they found that the trend of increasing spectral (blue) shifts as v_0 increases reverses at $v_0 = 40$,

indicating that for such high Br_2 vibrational states the vdW bond becomes stronger. Other experiments for the low v_0 region have been carried out by the Janda group [4,5], which have been compared with time independent [4] as well as time dependent [6] calculations.

In this article we review the theoretical work developed by the Madrid group on $HeBr_2$, focusing on the regime where Br_2 is close to the dissociation limit [7–10]. The close coupling method allows the calculation of excitation spectra and product distributions in a very efficient and accurate manner. A stabilisation method has also been applied and has been useful to uncover the details of the intramolecular dynamics. Comparisons with measurements [2–5] will be summarised and the sensitivity of the potential used will be briefly discussed.

II. THEORETICAL APPROACH: CLOSE-COUPLING AND STABILISATION METHODS

The partial cross section for the transition from a rovibrational bound state i of the electronic ground state X of $HeBr_2$ to a final dissociative state He + $Br_2(v_f, j_f)$ (v_f and j_f are the fragment vibrational and rotational levels) of the B electronic state is given by

$$\sigma_{i\to(v_f,j_f)}(E) \propto \omega \sum_{\Omega_f} \mid \langle \Psi_{fE}(B) \mid \boldsymbol{\mu}\cdot\boldsymbol{e} \mid \Psi_i(X)\rangle \mid^2, \tag{1}$$

where ω and $\boldsymbol{e}$ are the frequency and polarisation vector of the incident photon, respectively, $\boldsymbol{\mu}$ is the system dipole moment for the $(X \to B)$ transition, $\Psi_i(X)$ and $\Psi_{fE}(B)$ are bound and dissociative nuclear wave functions with energies E_i and E, respectively, $E = E_i + \hbar\omega$, and $f \equiv (v_f, j_f, \Omega_f)$, where Ω_f is the projection of the fragment angular momentum onto the body fixed axis.

The calculations are performed writing the X and B Hamiltonians in Jacobi coordinates $\boldsymbol{r}$ and $\boldsymbol{R}$, which are the vectors joining the two Br nuclei and the center of mass of Br_2 and the helium nucleus, respectively. The initial wave function $\Psi_i(X)$ is computed using standard variational methods. Two approaches are used for the calculation of the dissociative wave function: the close-coupling [7] and the stabilisation [8] methods.

In the close-coupling method, the B state wavefunction is written as

$$\Psi_{fE}^{JMp_ip_j}(\boldsymbol{R},\boldsymbol{r}) = \sum_{v,j,\Omega} \phi_{vj\Omega}^{fE}(R)\,\chi_v(r)\,\Theta_{j\Omega}^{JMp_ip_j}(\hat{\boldsymbol{r}},\hat{\boldsymbol{R}}), \tag{2}$$

where $\{\chi_v(r)\}$ are the vibrational wavefunctions for the isolated $Br_2(B)$ system, $\left\{\Theta_{j\Omega}^{JMp_ip_j}\right\}$ is a free rotor basis set [7,11], where J is the total angular momentum, M and Ω its projections onto the space and body fixed z axes respectively, p_i is the parity under nuclear coordinates inversion, and

p_j is the parity under bromine nuclei exchange. Eq. (2) is introduced into the Schrödinger equation and, after projection onto the basis functions for interhalogen and angular degrees of freedom, a close coupled system for the set of unknown functions $\phi^{fE}_{vj\Omega}(R)$ is obtained [11]. Such system is solved by means of a suitable propagation method [12], and applying standard boundary conditions for outgoing waves [11]. The quadrature involved in Eq. (2) is carried out by accumulation at the same time that the propagation is performed [13], so the continuum wave functions $\phi^{fE}_{vj\Omega}(R)$ are not explicitly obtained.

In the stabilisation method, the dissociative wave function is expanded in a set of square–integrable basis functions (as it were a bound state wave function)

$$\Phi_m^{JMp_ip_j}(\boldsymbol{R}, \boldsymbol{r}; \alpha) \;=\; \sum_{vkj\Omega} b^m_{vkj\Omega}(\alpha)\, \varphi_k(R;\alpha)\, \chi_v(r)\, \Theta^{JMp_ip_j}_{j\Omega}(\hat{\boldsymbol{r}}, \hat{\boldsymbol{R}}), \qquad (3)$$

where $\{\varphi_k(R;\alpha)\}$ constitute an orthonormal basis set depending on the parameter α. We used discrete variable representation functions obtained from diagonalisation of the R–coordinate operator in a primitive harmonic oscillator basis set. Dependence on the α parameter comes in the frequency parameter of the harmonic oscillator functions: $\omega = \sqrt{\alpha}\,\omega_0$, where ω_0 is a reference frequency. Varying α, the basis set functions span shorter or larger regions in the R-coordinate space. Following the approach of Mandelshtam *et al.* [14,15], the Hamiltonian is diagonalised for a large range of α values, obtaining a set of eigenvalues, E_m, and eigenfunctions, $\Phi_m^{JMp_ip_j}$, for each α. The total cross section is obtained by averaging the discrete form of the total cross section over α. The result is

$$< \sigma_i(E) > \approx (\Delta\alpha)^{-1} \sum_m \left| \frac{dE_m}{d\alpha} \right|^{-1}_{\alpha^*_m} \mid \langle \Phi_m(\alpha^*_m) \mid \boldsymbol{\mu}\cdot\boldsymbol{e} \mid \Psi_i(X) \rangle \mid^2, \qquad (4)$$

where α^*_m is the value where the $E_m(\alpha)$ curve intersects the constant line E.

Quasibound states can be distinguished by their stable behaviour, i.e., very small derivative $dE_m/d\alpha$ and, if the overlap involved in Eq. (4) is not too small, they cause a "bump" in the photofragmentation cross section. Then, such resonances can be studied by inspection of nodal patterns of the corresponding wave functions. This analysis contributes to the understanding of the underlying dynamics in the fragmentation process.

III. SUMMARY OF RESULTS

The potential energy surface used in our work is constructed as a sum of pairwise Br-Br and Br-He interactions. Morse parameters for the Br-He interaction were fitted [7] to reproduce, at low v_0 levels, experimental spectral shifts, lifetimes, and averaged structures [2,4]. Performance of this PES in the more intriguing region of high Br_2 vibrational levels is thus tested by comparing the results of the calculations with the available data.

One phenomenon successfully reproduced by calculations at high v_0 levels is the closing of the $\Delta v = -1$ channel for $v_0 \geq 44$. Due to the anharmonicity of the Br-Br stretching vibration the energy of one quantum of vibrational energy is no longer sufficient to dissociate the He atom from the Br_2 core, so that $v_f \leq v_0 - 2$ for $v_0 \geq 44$. It is thus interesting to investigate the dynamical behaviour below and above the closing of the one quantum channel. For $v_0 < 41$, we have found that the cross section profiles are well described by Lorentzian functions, indicating that the VP resonances are isolated. For $v_0 > 41$ such profiles become more and more structured. For example, the photofragmentation spectrum for the transition to $HeBr_2(B, v_0 = 45, J = 0)$ exhibits two maximum peaks of the same magnitude. This, together with the analysis of the product rotational distributions, which become quite structured near $v_0 = 44$, suggest the onset of important energy redistribution effects prior to dissociation.

Such intramolecular energy transfer mechanisms were more deeply investigated by means of stabilisation calculations for the $v_0 = 45$ level [8]. By inspection of the wavefunctions contributing most to the photofragmentation cross section, it is found that the intramolecular dynamics proceeds via coupling of the $HeBr_2(B, v_0 = 45)$ vdW ground state with a bending excited state belonging to the $v_0 - 1$ manifold; this intermediate state eventually couples with the dissociative continuum. This is, however, a too simplistic description of the dynamics, for there are also non negligible couplings with bound and continuum states of $v_0 - 1$ and $v_0 - 2$ and, additionally, such states also carry oscillator strength in the transition from the ground electronic state. Indeed, it is concluded that the vibrational excitation of the Br_2 subunit is no longer a good quantum number: as Br_2 and He-Br_2 vibrational frequencies become closer, the halogen subsystem does not retain its identity. New zero-order pictures (other than a diabatic separation of the faster halogen motion) should be devised to describe the intramolecular dynamics in this regime. An adiabatic approach could be an interesting alternative: the Hamiltonian matrix for degrees of freedom other than the interhalogen distance, r, is diagonalised for a range of r values and the resulting r-dependent eigenvalues act as perturbations of the free Br_2 interaction. A preliminary study has shown that this approach provides better zero-order quasibound state energies [9].

The prediction of important intramolecular vibrational redistribution (IVR) processes occurring in $HeBr_2(B, v_0 > 41)$ should be tested against experimental measurements. With that aim, a combined experimental and theoretical study of the rotational product distributions for $v_0 = 41$–48 levels has been carried out very recently [10]. A remarkable agreement between data and calculations was found for most vibrational levels. Very interestingly, a qualitative change in the shape of the rotational distributions has been found when IVR becomes dominant ($v_0 > 44$). This result places $HeBr_2$ as the second triatomic rare gas-halogen vdW molecule for which IVR has been shown to be important (the first one is $ArCl_2$ [16]).

One important conclusion of these studies is that the very simple potential model used successfully reproduces most of the experimental data in the whole range of vibrational excitations $v_0 = 8$–48 (average structures, spectral shifts, linewidths, product rotational distributions). In addition, we have found good agreement with data for the vibrational energy transfer in the He + $Br_2(B)$ collision [17]. However, some measurements for high vibrational levels are not satisfactorily simulated by the theory: the product distributions right at the closing of the $\Delta v = -1$ channel ($v_0 = 43, 44$) (which are very sensitive to the potential), and more importantly, the large increase in the vdW dissociation energy when $v_0 > 40$. Therefore, the present potential should be regarded as a good reference for further improvements in the PES in the region of very large interhalogen separations. In this context, application of the Diatomics in Molecules (DIM) approach, that explicitly extends to the proper He-Br potential for large Br-Br separations, can be very useful and insightful [18]. We can expect that progress in this direction together with new detailed measurements will eventually lead to a complete determination of the potential energy surface.

ACKNOWLEDGMENTS

Some parts of this project have been developed in collaboration with A. A. Buchachenko from Moscow State University, Russia and A. Rohrbacher, T. Ruchti, K. C. Janda from University of California at Irvine, USA.

[1] See, for example, K. C. Janda and C. R. Bieler, in *Atomic and Molecular Clusters*, edited by E. R. Berstein, p.455 (Elsevier, Amsterdam, 1990).
[2] L. J. van de Burgt, J. P. Nicolai, M. C. Heaven, J. Chem. Phys. **81**, 5514 (1984).
[3] D. G. Jahn, S. G. Clement, K. C. Janda, J. Chem. Phys. **101**, 283 (1994).
[4] D. G. Jahn, W. S. Barney, J. Cabalo, S. G. Clement, T. J. Slotterback, K. C. Janda, N. Halberstadt, J. Chem. Phys. **104**, 3501 (1996).
[5] N. Sivakumar, J. I. Cline, C. R. Bieler, K. C. Janda, Chem. Phys. Lett. **147**, 561 (1988).
[6] P. J. Krause and D. C. Clary, Chem. Phys. Lett, **271**, 171 (1997).
[7] T. González–Lezana, M. I. Hernández, G. Delgado–Barrio, A. A. Buchachenko and P. Villarreal, J. Chem. Phys. **105**, 7454 (1996).

[8] T. González–Lezana, M. I. Hernández, G. Delgado–Barrio and P. Villarreal, J. Chem. Phys. **106**, 3216 (1997).
[9] T. González–Lezana, M. I. Hernández, G. Delgado–Barrio and P. Villarreal, J. Mol. Struct. (Theochem), in press (1998).
[10] A. Rohrbacher, T. Ruchti, K. C. Janda, A. A. Buchachenko, M. I. Hernández, T. González–Lezana, Pablo Villarreal and G. Delgado-Barrio, J. Chem. Phys. (to be submitted).
[11] O. Roncero, J. A. Beswick, N. Halberstadt, P. Villarreal and G. Delgado–Barrio, J. Chem. Phys. **92**, 3348 (1990).
[12] L. Fox, *The Numerical Solution of Two–Point Boundary Value Problems in Ordinary Differential equations* (Clarendon P, 1957).
[13] O. Roncero, private communication.
[14] V. A. Mandelshtam, T. R. Ravuri and H. S. Taylor, Phys. Rev. Lett. **70**, 1932 (1993).
[15] V. A. Mandelshtam, T. R. Ravuri and H. S. Taylor, Phys. Rev. A **48**, 818 (1993).
[16] D. D. Evard, C. R. Bieler, J. I. Cline, N. Sivakumar and K. C. Janda, J. Chem. Phys. **89**, 2829 (1988).
[17] A. A. Buchachenko, T. González-Lezana, M. I. Hernández, G. Delgado-Barrio, P. Villarreal and N.F. Stepanov, Chem. Phys. Lett. **269**, 448 (1997).
[18] A.A. Buchachenko and N.F. Stepanov, J. Chem. Phys. **106** 10134 (1997).

R. Prosmiti, J. Tennyson, D. C. Clary (eds.)
Molecular Quantum States at Dissociation

Regular and Irregular Vibrational Wavefunctions of Ar_3

Nicholas J. Wright and Jeremy M. Hutson
Department of Chemistry, University of Durham, South Road, Durham, DH1 3LE, UK

I. INTRODUCTION

The coupling of molecular beam techniques with laser technology has led to the development of powerful experimental techniques for probing highly excited states of molecules [1]. The results of such experiments present a major challenge to theory. The "traditional" approach of predicting spectra from an effective Hamiltonian based on normal mode analysis no longer works, because the large-amplitude motions characteristic of highly excited states invalidate any approach based upon small deviations from a reference geometry.

A more general way to understand spectra is to solve the Schrödinger equation exactly using a global potential energy surface. Unfortunately both the determination of the potential energy surface and the solution of the Schrödinger equation present major challenges in their own right. However, the approach can be followed for prototype systems, and it is interesting to examine the wavefunctions that are obtained.

Traditionally, quantum numbers would be assigned to vibrational wavefunctions using a normal mode approach. If the equilibrium geometry and force constants are known, group theory can be used to determine the normal modes. It is then possible to determine the degree of excitation in each mode by examining each wavefunction in turn, starting from the ground state and working upwards.

The problem with this procedure is that the approximation it is based upon, that of small-amplitude uncoupled vibrations in the different modes, breaks down as the molecule becomes more and more excited. The energy at which the breakdown begins depends on the potential energy surface of the molecule and the masses of the atoms. For a chemically bound molecule such as HCP, the breakdown begins approximately 20,000 cm^{-1} above the minimum of the potential energy surface [2]. In H_3^+ it begins approximately 12,000 cm^{-1} above the minimum [3]. For a Van der Waals molecule such as Ar_3 the breakdown is much more rapid and occurs approximately 100 cm^{-1} above the potential minimum.

When the wavefunctions can no longer be assigned in terms of normal modes they begin to enter a totally different regime. Many of the wavefunctions for higher-lying states are irregular and show no recognisable structure. However, lying among the irregular states are often others with quite regular wavefunctions, which may be localised in the vicinity of classical periodic orbits. Such orbits are (classical) trajectories that describe closed figures in phase space, so that after some time t the classical system has exactly the same position and momentum as before. (For more details, see Refs. [4–6].) Such localisation of quantal wavefunctions has been observed in H_3^+ [7,8], HCN [9] and HCP [2]. Our work is similar in concept, but has concentrated on the Ar_3 Van der Waals molecule. Both Ar_3 and H_3^+ have an equilateral triangle equilibrium geometry and therefore some similarities between Ar_3 and H_3^+ are to be expected; on the other hand, the masses and energy scales are quite different, so the extent of the similarities and differences is interesting.

II. WAVEFUNCTIONS OF Ar_3

We have calculated the wavefunctions for the $J = 0$ states of Ar_3, using a high-quality pairwise-additive potential energy surface and a potential-optimised discrete variable representation (PO-DVR) method [10]. Some representative results are shown in Fig. 1. The wavefunctions are calculated in Jacobi coordinates, and are a function of all three variables R, r and θ. However, the features we wish to highlight are most clearly seen in 2-dimensional cuts with the angle θ fixed at 90°, which is the configuration shown in Fig. 1. The top two panels of the figure show the ground-state wavefunction and the potential energy surface.

Most of the wavefunctions have no regular features at all, with no clear nodal structure; an example of this is shown in Fig. 1b. The solid boundary outlines the classically allowed region of configuration space at the energy of the eigenstate, and it may be seen that the wavefunction in Fig. 1b fills almost all the available configuration space.

Other wavefunctions are more regular. For example, Fig. 1c shows the wavefunction for another state, quite close in energy to that in Fig. 1b, but of a completely different character. This is a "horseshoe" state, so called because it is localised along a line that appears horseshoe-shaped if the figure is extended to include the reflection to negative R. Similar states have been observed in H_3^+ [7]. The horseshoe motion can be visualised as involving one argon atom moving through and perpendicular to the (vibrating) Ar_2 bond.

The regular motion shows the influence of a classical periodic orbit upon the wavefunction. Instead of filling all the energetically accessible configuration space, the horseshoe state samples only a distinct subspace, and the nodal lines (planes) are mostly perpendicular to the path of the periodic orbit.

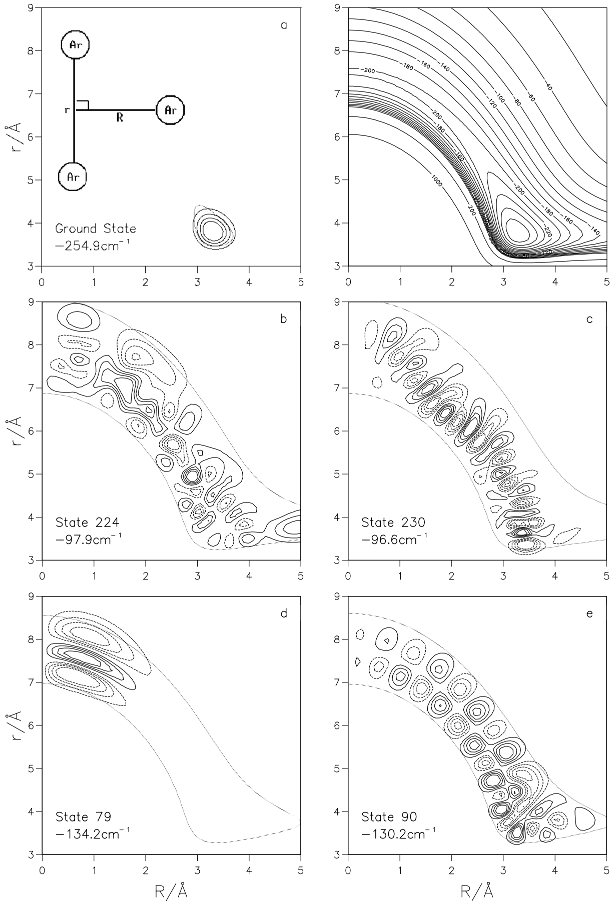

FIG. 1. The potential energy surface and wavefunctions of Ar_3 plotted in the coordinate system shown. The solid boundary line denotes the classically allowed region of configuration space at the energy of the eigenvalue. Dashed and solid contours show negative and positive values of the wavefunction respectively. Contours are for 0.64, 0.48, 0.32 and 0.16 of the maximum amplitude.

The horseshoe states are not the only regular states that exist. The wavefunction in Fig. 1d resembles that for the symmetric bending mode of a bent triatomic molecule. This particular state has 2 quanta of excitation in this “mode”. States with different degrees of excitation are also observable. Fig. 1e shows a state similar to the ‘nodal horseshoe’ state described in Ref. [8]. This is a combination of the two localised “modes” described above, suggesting that they can be combined in a manner similar to normal modes.

A common feature of the localisation effects observed is that the “regular” character is often distributed over several nearby eigenstates. To label one particular state as *the* horseshoe state, for example, is often impossible. This accords with the standard “time-independent” picture of intramolecular vibrational energy redistribution [11]: when a regular state is embedded in a dense “bath” of other states, the character of the regular state is spread out over the bath states, its contribution peaking as a function of energy in a near-Lorentzian manner. At higher energies, the density of “bath” states is greater and the “regular” character is spread over more energy levels. If the bath is dense enough, it may turn out that no one eigenstate ends up with a significant amount of “regular” character. Such effects can be thought of as the bound state analogue of quantum mechanical scattering resonances. When the quasi-continuum becomes an actual (dissociative) continuum, the regular character is spread out over the width of the resulting predissociating state.

The wavefunctions of floppy molecules reveal a fascinating range of dynamical behaviour. Future work in this area should lead to a better understanding of the relationship between the quantum and classical descriptions of such systems. At the moment it is possible to calculate the wavefunctions and explain their localisation features with reference to the periodic orbits of the system. A theory in which one calculates the periodic orbits and then predicts which one, or which family, leads to quantum localisation is not yet available. However, by studying a range of different molecules, it may be possible to develop such a theory.

---

[1] D. J. Nesbitt, “High-resolution, direct infrared laser absorption spectroscopy in slit supersonic jets: Intermolecular forces and unimolecular vibrational dynamics in clusters”, Ann. Rev. Phys. Chem. **45**, 367 (1994).

[2] C. Beck, H. Keller, S. Y. Grebenshchikov, R. Schinke, S. C. Farantos, K. Yamashita and K. Morokuma, “Highly excited vibrational states of HCP and their analysis in terms of periodic orbits: The genesis of saddle-node states and their spectroscopic signature”, J. Chem. Phys. **107**, 9818 (1998).

[3] D. A. Sadovski, N. G. Fulton, J. R. Henderson, J. Tennyson and B. I. Zhilinskiĭ, “Nonlinear normal modes and local bending vibrations in H_3^+ and D_3^+”, J. Chem. Phys. **99**, 906 (1993).

[4] J. M. Gomez Llorente and E. Pollak, “Classical dynamics methods for high energy vibrational spectroscopy”, Ann. Rev. Phys. Chem. **43**, 91 (1992).

[5] S. C. Farantos, “Exploring molecular vibrational motions with periodic orbits”, Int. Rev. Phys. Chem. **15**, 345 (1996).

[6] E. J. Heller, in *Les Houches Lectures LII: Chaos and quantum physics*. M. J. Giannoni, A. Voros, and J. Zinn-Justin, (eds), p.547, (North-Holland, 1991).

[7] G. García de Polavieja, N. Fulton and J. Tennyson, “Coarse grained spectra, dynamics and quantum phase space structures of H_3^+”, Mol. Phys. **83**, 361 (1994).

[8] G. García de Polavieja, N. Fulton and J. Tennyson, "Quantum transport, recurrence and localisation in H_3^+", Mol. Phys. **87**, 651 (1996).
[9] S. C. Farantos, J. M. Gómez Llorente, O. Hahn and H. S. Taylor, "The extraction of dynamics and the classical mechanical simulation of low resolution regular and chaotic spectra: HCN/HNC", J. Chem. Phys. **93**, 76 (1990).
[10] N. J. Wright and J. M. Hutson, "Ar_3: A quantum mechanical study", in preparation.
[11] M. Bixon and J. Jortner, "Long radiative lifetimes of small molecules", J. Chem. Phys. **50**, 3284 (1969).

R. Prosmiti, J. Tennyson, D. C. Clary (eds.)
Molecular Quantum States at Dissociation

The Effect of Rotation on Resonances

Joel M. Bowman
Department of Chemistry and Cherry L. Emerson Center for Scientific Computation, Emory University, Atlanta, GA 30322, USA

Resonances are metastable states of a molecular complex. They are formed in many cases by vibrational excitation of a molecular complex above a dissociation threshold. This excitation can be (and statistically is most often) in vibrational modes not associated with dissociation. Thus, the lifetime of the complex can be many periods of an average vibration. The decay of a resonance is due to the coupling between excited modes and the dissociation mode(s), and thus our understanding of resonance properties is challenged by the non-linear dynamics in the high energy (and possibly chaotic) region of the spectrum.

However, because of their long lifetimes, resonances share a number of features in common with ordinary bound states, including the possibility of making spectroscopic assignments of them. In particular, in understanding the effect of overall rotation on resonance properties, we and others have shown that there is a strong correspondence with the rotational properties of bound states.

Before proceeding with a brief review of some investigations of the effect of rotation on resonances, it is worth noting the place in kinetics where such information is of importance. The well-known RRKM expression for the microcanonical unimolecular rate constant is the microcanonically averaged decay rate, summed over states of total angular momentum. To obtain this rate rigorously from a dynamics calculation requires a calculation of the decay rates as a function of total angular momentum, which immediately returns us to the subject of this short review, which will focus on the radical, HCO.

Resonances in HCO, a radical of importance in combustion, have been studied and characterised by us and other groups for a number of years [1–7]. More recently, the effect of rotation on these resonances has been examined by four groups [1][d,e], [3][b], [6][d], [7]. In these studies, it was found that the dependence of the resonance energies of HCO, which is a near prolate symmetric top, can be well approximated by the simple expression

$$E_i^{J,K} = E_i^{J=0} + \overline{B}_i J(J+1) + (A_i - \overline{B}_i)K^2, \tag{1}$$

where $E_i^{J=0}$ is the energy of the ith resonance for zero total angular momentum, and $\overline{B}_i$ and A_i are corresponding rotation "constants", which depend on "i", the resonance state label. (As usual, $\overline{B}$ is the average of the B and C rotation constants.) The resonance widths also showed a similar dependence on J and K, the usual body-fixed projection quantum number of J; however, with constants *not* equal to $\overline{B}_i$ and A.

This remarkably simple dependence of resonance energies and widths on J and K led us to consider applying and testing an approximate treatment of rotation that we have termed the Adiabatic Rotation Approximation. In this approximation the Hamiltonian is given by

$$H^J = H^{J=0} + E^J(Q), \tag{2}$$

where $H^{J=0}$ is the full Hamiltonian for $J = 0$ (which contains a negative imaginary, absorbing potential in our applications), and $E^J(Q)$ is the adiabatic rotational energy for the nuclear configuration denoted by Q, the collection of $3N$-6 internal coordinates. In general this energy is obtained by diagonalisation of the inertia tensor and solution of the usual Schrödinger equation for the rotational motion. The procedure simplifies for (near) symmetric tops, where K is also a good quantum number. In this case $E^J(Q)$ is given by the usual symmetric top expression, and

$$H^{J,K} = H^{J=0} + \overline{B}J(J+1) + (A - \overline{B})K^2, \tag{3}$$

where now $\overline{B}$ and A are the rotation "constants" in the "instantaneous" principal axis system, and thus they are functions of the nuclear coordinates. The rotational energy is added to the electronic potential energy surface(s) to form an effective potential. This simplified, but very useful form of the adiabatic rotation Hamiltonian had been used by us in approximate quantum reactive scattering calculations [8], and twenty years ago it was suggested by McCurdy and Miller (and which they termed the Principal Axis Helicity Conserving Approximation) in the context of a semi-classical Hamiltonian [9]. Miller and co-workers applied this approximation with very good success to the direct calculation of rate constants [10]. Very recently, Miller and co-workers have applied this approximation to the $H+O_2$ reaction; however, they used an approximate principal-axis system given by the Jacobi coordinates for the O_2-H arrangement channel in which the body-fixed top axis is the OO bond-axis [11]. (Although this is the best choice for Jacobi coordinates, we showed earlier for HCO that making the analogous choice for the top axis, i.e., the CO bond-axis, the results were not quite as accurate as using the exact principal-axis system [12].)

I. PERTURBATION THEORY

Our tests [1][e] and those of Yang and Gray [3][b] of the adiabatic rotation approximation for HCO and other tests by Miller and co-workers [10] have established that this approximation does provide an accurate description

of overall rotation (the one caveat being the neglect of coriolis coupling). Thus, we thought it would be fruitful to treat the adiabatic rotational energy as a perturbation in order to develop some qualitative understanding of the effect of rotation on resonances [12]. Doing so, to first order, gives the usual expression for the the shift in the $J = 0$ *complex* resonance energies

$$\langle \chi_n^{(0)} | E^J(Q) | \chi_n^{(0)} \rangle, \tag{4}$$

where $\chi_n^{(0)}$ is the complex eigenfunction of $H^{J=0}$ for the nth resonance. This complex energy shift, denoted $\Delta\varepsilon_n^{(J)}$, can be written as

$$\Delta\varepsilon_n^{(J)} = \Delta E_n^{(J)} - \frac{i}{2}\Delta\Gamma_n^{(J)}, \tag{5}$$

where $\Delta E_n^{(J)}$ and $\Delta\Gamma_n^{(J)}$ are the shifts in the position and width of the resonance.

For a symmetric top, E^J is given by the usual expression, and thus

$$\Delta\varepsilon_n^{(J,K)} = \langle \chi_n^{(0)} | \overline{B} | \chi_n^{(0)} \rangle J(J+1) + \langle \chi_n^{(0)} | A - \overline{B} | \chi_n^{(0)} \rangle K^2. \tag{6}$$

If we write $\chi_n^{(0)}$ in terms of its real and imaginary parts, $\phi_n^{(0)}$ and $\pi_n^{(0)}$, respectively, we have

$$\begin{aligned} \Delta E_n^{(1)} &= \overline{B}_n^{(0)} J(J+1) + (A_n^{(0)} - \overline{B}_n^{(0)})K^2 \\ -\frac{\Delta\Gamma_n^{(1)}}{4} &= \overline{\beta}_n^{(0)} J(J+1) + (\alpha_n^{(0)} - \overline{\beta}_n^{(0)})K^2, \end{aligned} \tag{7}$$

where

$$\overline{B}_n^{(0)} \equiv \langle \phi_n^{(0)} | \overline{B} | \phi_n^{(0)} \rangle - \langle \pi_n^{(0)} | \overline{B} | \pi_n^{(0)} \rangle, \tag{8a}$$
$$A_n^{(0)} \equiv \langle \phi_n^{(0)} | A | \phi_n^{(0)} \rangle - \langle \pi_n^{(0)} | A | \pi_n^{(0)} \rangle, \tag{8b}$$
$$\overline{\beta}_n^{(0)} \equiv \langle \pi_n^{(0)} | \overline{B} | \phi_n^{(0)} \rangle, \tag{8c}$$
$$\alpha_n^{(0)} \equiv \langle \pi_n^{(0)} | A | \phi_n^{(0)} \rangle. \tag{8d}$$

Thus, to first order, the shifts in both the positions *and* widths scale with J and K according to the symmetric top expression. For resonances, the real part of $\chi_n^{(0)}$ is generally much larger than that of the imaginary part, and so, in general, $\overline{B}_n^{(0)}$ and $A_n^{(0)}$ are positive. Thus the shifts in the resonance positions are positive, as expected. However, the shifts in the widths may be positive, zero, or negative, because the constants $\overline{\beta}_n^{(0)}$ and $\alpha_n^{(0)}$ may be of any sign or approximately zero. (For bound states the energies and zero-order wavefunctions are real and so the imaginary part of $\Delta\varepsilon_n^{(J,K)}$ is zero.)

Thus, perturbation theory provides at least a qualitative framework to understand the behaviour of the shifts in positions and widths of resonances with respect to overall rotation. Of course, the validity of this framework depends on the validity of first-order perturbation theory. We have tested this and found the accuracy to be as expected, i.e., accurate for small shifts in resonance energies and widths, and less accurate as these increase.

HCO is atypical of most stable molecules in that it has only a small number (fifteen) of bound states. And while much has been learned from studies of resonances in this system (including detailed comparisons with experiment), more studies of resonances and comparisons with experiment need to be done for molecules with many more bound states. This is being done, in a comprehensive multi-group collaboration, for HOCl. The calculations include the creation of a global potential based on very high quality *ab initio* calculations of the electronic energies, and calculations of the bound and resonance states for zero and non-zero total angular momentum [13]. These calculations were stimulated in part by recent high resolution experiments measuring the dissociation lifetimes of HOCl from high OH overtones and specific J and K states [14,15]. The experiments indicate highly non-statistical lifetime distributions.

Thus far we have fit and slightly adjusted a potential surface based on high quality MRCI *ab initio* electronic structure calculations of Peterson [13]^a. We along with Yang and Gray and Mandleshtam have determined all of the bound states of non-rotating HOCl and we have also performed extensive calculations for $J > 0$ [13]^b. These include exact calculations which have enabled a test of the adiabatic rotation approximation, which we find to be very accurate for this molecule, which like HCO is a near prolate top. The spectrum has been characterised as Poisson [13]^b, which is in sharp contrast to the spectrum of other triatomics, e.g., H_3^+ [16], which have been characterised as Wigner.

In summary, the study of resonances indicates that resonances have some features in common with ordinary bound states, including the effect of rotation on resonance energies. However, resonances have been studied far less than bound states and further work, both theoretical and experimental, is needed to put our understanding of them on a firm foundation.

[1] (a) K. T. Lee and J. M. Bowman, J. Chem. Phys. **86**, 215 (1987); (b) S. W. Cho, A. F. Wagner, B. Gazdy and J. M. Bowman, J. Chem. Phys. **96**, 2812 (1992); (c) D. Wang and J. M. Bowman, J. Chem. Phys. **100**, 1021 (1994); (d) D. Wang and J. M. Bowman, Chem. Phys. Lett. **235**, 277 (1995); (e) J. Qi and J. M. Bowman, J. Chem. Phys. **105**, 9884 (1996); (f) J. M. Bowman, J. Phys. Chem. **102**, 3006 (1998).

[2] R. N. Dixon, J. Chem. Soc. Farad. Trans. **88**, 2575 (1992).

[3] (a) S. K. Gray, J. Chem. Phys. **96**, 6543 (1992); (b) C.-Y. Yang and S. K. Gray, J. Chem.

Phys. **107**, 7773 (1997).

[4] V. Ryaboy and N. J. Moiseyev, Chem. Phys. **103**, 4061 (1995).

[5] T. P. Grozdanov, V. A. Mandelshtam and H. S. Taylor, J. Chem. Phys. **103**, 7990 (1995).

[6] (a) H.-J. Werner, C. Bauer, P. Rosmus, H.-M. Keller, M. Stumpf and R. Schinke, J. Chem. Phys. **102**, 3593 (1995); (b) H.-M. Keller, H. Flöthmann, A. J. Dobbyn, R. Schinke, H.-J. Werner, C. Bauer and P. Rosmus, J. Chem. Phys. **105**, 4983 (1996); (c) H.-M. Keller, M. Stumpf, T. Schroeder, C. Stoeck, F. Temps, R. Schinke, H.-J. Werner, C. Bauer and P. Rosmus, J. Chem. Phys. **106**, 5359 (1997); (d) H. M. Keller and R. Schinke, J. Chem. Soc., Farad. Trans. **93**, 879 (1997).

[7] G. S. Whittier and J. C. Light, J. Chem. Phys. **107**, 1816 (1997).

[8] D. Wang and J. M. Bowman, J. Phys. Chem. **98**, 7994 (1994).

[9] C. W. McCurdy and W. H. Miller, in *A New Helicity Representation for Reactive Atom-Diatom Collisions*, edited by P.R. Brooks and E. F Hayes, **56**, (ACS, 1977).

[10] (a) H. Wang, W. H. Thompson and W. H. Miller, J. Chem. Phys. **107**, 7194 (1997); (b) W. H. Thompson and W. H. Miller, J. Chem. Phys. **106**, 142 (1997); (c) T. C. Germann and W. H. Miller, J. Phys. Chem. **101**, 6358 (1997).

[11] D. E. Skinner, T. C. Germann and W. H. Miller, J. Phys. Chem., in press, (1998).

[12] J. Qi and J. M. Bowman, J. Chem. Phys. **107**, 9960 (1997).

[13] (a) S. Skokov, J. M. Bowman and K. A. Peterson, J. Chem. Phys., in press, (1998); (b) S. Skokov, J. Qi, C-Y. Yang, J. M. Bowman, S. K. Gray, K. A. Peterson and V. Mandelshtam, "Accurate variational calculations and characterization of the HOCl bound vibrational state spectrum", to be published.

[14] R. J. Barnes and A. Sinha, J. Phys. Chem. **A101**, 8374 (1997).

[15] M. R. Wedlock, R. Jost and T. R. Rizzo, J. Chem. Phys. **107**, 10344 (1997).

[16] V. A. Mandelshtam and H. S. Taylor, J. Chem. Soc., Farad. Trans. **93**, 847 (1997).

R. Prosmiti, J. Tennyson, D. C. Clary (eds.)
Molecular Quantum States at Dissociation

Time-Dependent Study of Resonances

John Z. H. Zhang
Department of Chemistry, New York University, New York, NY 10003, USA

One of the most important results of quantum scattering theory is the phenomenon of resonance. Resonance plays important roles in bimolecular collision and unimolecular reaction. For example, the product branching ratio and product state distribution in a bimolecular reaction or unimolecular dissociation are often controlled by resonance states. The resonance states are also called metastable species in chemistry and their existence can be detected and lifetimes can be measured experimentally by spectroscopic and other methods. The formation of resonance states or metastable species can arise from a variety of energy transfer processes such as bimolecular collision, photoabsorption, or other energetic processes [1]. The theoretical treatment of resonance is a difficult task partly because resonance states are not as well defined as bound states. Rigorously speaking, resonance states are continuum states that possess some bound state characteristics such as locality [2]. The properties of resonance states can vary widely from those that are essentially continuum scattering states to those that behave almost like bound states depending on their relative lifetimes.

Time-dependent (TD) wavepacket approach provides an attractive means for calculating quantum resonance states, especially for large scale molecular calculations. An important advantage of the TD approach is that one does not need to diagonalise or invert the Hamiltonian matrix as is required in traditional time-independent approaches to calculating bound and scattering problems. As a result, the computational time in TD approach is proportional to N^α ($1< \alpha <2$) — where N is the size of the Hamiltonian matrix — rather than N^3 as in standard methods of matrix diagonalisation or inversion. This makes the TD approach a powerful computational tool for large scale calculation of molecular states.

Theoretical methods to calculate quantum resonances are divided into two general categories: (1) bound state approach and (2) scattering state approach. In bound state approach to resonance, one treats resonance states as quasi-bound states with complex energies and solves the complex eigenvalue problems [3,4]. In the more rigorous scattering state approach, one solves the scattering problem to obtain the energy-dependence of scattering matrices from which to extract resonance information such as position and width of resonances. Both approaches can be efficiently carried out by TD wavepacket method.

In the bound state TD approach to resonance, one carries out wavepacket propagation from any chosen initial wavepacket $\psi(0)$ with the absorbing boundary condition [5–8]. The application of absorbing boundary condition is to damp out continuum state contribution to the spectrum. By Fourier transforming the autocorrelation function $A(t) = \langle\psi(0)|\psi(t)\rangle$, one obtains the energy spectrum in which resonance states appear as spectral peaks and positions of these peaks correspond to resonance energies. The resonance wavefunction can also be obtained by performing a straightforward time $\rightarrow$ energy Fourier transform on the TD wavefunction $\psi(t)$. The resonance widths can be extracted from the TD calculation by a number of means. For isolated resonance, one can simply fit the resonance spectrum to the Breit-Wigner formula. Alternatively, one may choose to calculate the decay rate of the resonance wavefunction by propagating the resonance wavefunction in time. For very long-lived resonances one could use the Prony method to directly fit the autocorrelation to resonance formula [5]. In another approach [6], one could artificially broaden the resonance width by using a Lorentzian window function in Fourier transforming the autocorrelation function to spectrum.

In the scattering state TD approach to resonance, the basic method is very similar to that in bound state approach. However, since one solves a complete scattering problem, one usually chooses an initial wavepacket located in the asymptotic region of the reagent. In addition, the initial wavepacket usually corresponds to a pure internal (rovibraitonal) eigenstates of the colliding molecules. The scattering calculation can be complicated if reaction or rearrangement occurs which is often the case in chemical dynamics. Absorbing boundary condition is also applied in the scattering calculation in order to limit the range of numerical grid. The resonance states are then identified from the energy-dependence of calculated reaction probability or scattering matrix [9]. The computational cost is certainly higher than that in bound state approach but one obtains more detailed dynamical information from such calculations.

The above two approaches are complimentary with the scattering state approach being more rigorous but computationally more challenging.

---

[1] See *Resonances*, ACS Symp. Ser. 263, edited by D. G. Truhlar (1984).
[2] C. L. Shoemaker, and R. E. Wyatt, Ad. Quant. Chem., **14**, 169 (1981).
[3] V. A. Mandelshtam and H. S. Taylor, in *Dynamics of Molecules and Chemical Reactions*, edited by R. E. Wyatt and J. Z. H. Zhang (Marcel Dekker, New York, 1996).
[4] J. Qi and J. M. Bowman, J. Chem. Phys. **100**, 15165 (1996); D. Wang and J. M. Bowman, Chem. Phys. Lett. **235**, 277 (1995).

[5] S. K. Gray and C. E. Wozny, J. Chem. Phys. **91**, 7671 (1989); **94**, 2817 (1991).
[6] J. Dai and J. Z. H. Zhang, J. Chem. Phys. **103**, 1491 (1995).
[7] J. Dai and J. Z. H. Zhang, J. Chem. Phys. **104**, 3664 (1995).
[8] V. A. Mandelshtam, T. P. Grozdanov, and H. S. Taylor, J. Chem. Phys. **103**, 10074 (1995).
[9] D. H. Zhang and J. Z. H. Zhang, J. Chem. Phys. **101**, 3671 (1994).

R. Prosmiti, J. Tennyson, D. C. Clary (eds.)
Molecular Quantum States at Dissociation

Electronically Non-adiabatic Dynamics and Resonance Lifetimes

Donald G. Truhlar
Department of Chemistry and Supercomputer Institute, University of Minnesota, Minneapolis, MN 55455-0431, USA

The development of practical, yet accurate methods for the treatment of photochemical reactions (i.e., reactions of electronically excited species) and for the treatment of non-adiabatic dissociation of electronically excited resonance states is a challenging problem. In recent years we have developed the capability for calculating accurate quantum mechanical transition probabilities for electronically adiabatic atom-diatom collisions and the decay of resonance states of triatomic complexes when the coupled potential energy surfaces of these systems are assumed known in a diabatic representation [1–5]. This allows us to test simple models (of, for example, the effect of changing the location of a crossing seam on the extent of vibrational excitation of the products) against the accurate results.

We are engaged in several projects addressing questions in the quantum mechanical and semiclassical treatment of electronically non-adiabatic molecular processes. We are studying the creation of practical diabatic representations and their use for converged quantum dynamics calculations. We have developed an accurate diabatic potential set for NaFH [6] and an improved diabatic potential set for NaH_2 [7]. In both cases the potentials are based on accurate *ab initio* calculations of adiabatic potential surfaces, and the fits are based on valence bond configuration mixing models. We have found that our new potential energy surface set for NaFH leads to good agreement with experiment for photo-depletion of NaFH Van der Waals molecules [8].

We are also testing the accuracy of nonadiabatic transition state theory and existing trajectory surface hopping and self-consistent potential methods applied to unimolecular lifetimes and product distributions for decay of metastable exciplex resonances [9–12] and applied to state-to-state transition probabilities in bimolecular collisions [13–15]. We have tested semiclassical methods against accurate quantum dynamics for the following cases of electronically non-adiabatic processes:

1. Na(3p) + H_2 $\rightarrow$ Na(3s) + vibrationally-rotationally excited H_2 [9,13–15]
2. Na(3p) + H_2 $\rightarrow$ NaH + H [14,15]
3. NaH_2^* $\rightarrow$ Na(3s) + H_2 [12]

4. $NaFH^* \to Na + HF$ or $NaF + H$ [10]
5. $Br^* + H_2 \to Br + H_2$ or $HBr + H$ [11]
6. Model systems similar to 2 and 4, but designed to allow comparison of endothermic and exothermic reactions [15].

We have found that semiclassical methods for electronically non-adiabatic processes are less accurate, in general, than quasiclassical trajectory methods for electronically adiabatic processes [15]. Based on these studies, we are proposing new semiclassical algorithms with improved performance.

In another set of projects related to the subject of this workshop, we have been developing new methods for calculating accurate quantum mechanical lifetimes of very-long-lived states of four-body complexes. Preliminary results [16] for the HF dimer [17] obtained by the analytic continuation of real stabilisation graphs [18] are very encouraging.

ACKNOWLEDGMENTS

I am very grateful to my collaborators listed in the references and unpublished projects listed below. This work is supported in part by the U. S. National Science Foundation.

---

[1] S. L. Mielke, G. J. Tawa, D. G. Truhlar and D. W. Schwenke, "Energy Transfer through Exciplex Funnel States", J. Am. Chem. Soc. **115**, 6436 (1993).

[2] S. L. Mielke, G. J. Tawa, D. G. Truhlar and D. W. Schwenke, "Partial Widths of Feshbach Funnel Resonances in the Na(3p)H_2 Exciplex", Int. J. Quant. Chem. Symp. **27**, 621 (1993).

[3] S. L. Mielke, G. J. Tawa, D. G. Truhlar and D. W. Schwenke, "Quantum Photochemistry. Accurate Quantum Scattering Calculations for an Electronically Nonadiabatic Reaction", Chem. Phys. Lett. **234**, 57 (1995).

[4] S. L. Mielke, D. G. Truhlar and D. W. Schwenke, "Quantum Photochemistry. The Competition Between Electronically Nonadiabatic Reaction and Electronic-to-Vibrational, Rotational, Translational Energy Transfer in Br^* Collisions with H_2", J. Phys. Chem. **99**, 16210 (1995).

[5] T. C. Allison, S. L. Mielke, D. W. Schwenke and D. G. Truhlar, "Funnel States as Mediators of Born-Oppenheimer Breakdown in Reactions at an Avoided Crossing", J. Chem. Soc., Farad. Trans. **93**, 825 (1997) (Special issue on Quantum Theory of Chemical Reactions).

[6] M. S. Topaler, D. G. Truhlar, X. Y. Chang, P. Piecuch and J. C. Polanyi, "Potential Energy Surfaces of NaFH", J. Chem. Phys. **108**, 5349 (1998).

[7] M. D. Hack and D. G. Truhlar, "Potential Energy Surfaces and their couplings for the Electronically Nonadiabatic Chemical Reaction Na(3p) + H_2", to be published.

[8] M. S. Topaler, D. G. Truhlar, X. Y. Chang, P. Piecuch and J. C. Polanyi, "The Photoabsorption Spectrum of Na $\cdots$ FH van der Waals Molecule. Comparison of Theory and Experiment for a Harpooning Reaction Studied by Transition State Spectroscopy", J. Chem. Phys. **108**, 5378 (1998).

[9] M. S. Topaler and D. G. Truhlar, "Statistical Model for Nonadiabatic Decay of an Exciplex Strongly Coupled to a Dissociative Continuum", J. Chem. Phys. **107**, 392 (1997).

[10] Y. Zeiri, G. Katz, R. Kosloff, M. S. Topaler, J. C. Polanyi and D. G. Truhlar, "Deep Quantum Photophysics", to be published.

[11] Y. L. Volobuev, M. D. Hack and D. G. Truhlar, "Comparison of Semiclassical and Quantum Mechanical Methods for Br^* Collisions with Hydrogen Molecule", to be published.

[12] M. D. Hack and D. G. Truhlar, "Comparison of Semiclassical and Quantum Mechanical Methods for the Decay of NaH_2^* Exciplexes", to be published.

[13] M. S. Topaler, M. D. Hack, T. C. Allison, Y.-P. Liu, S. L. Mielke, D. W. Schwenke and D. G. Truhlar, "Validation of Trajectory Surface Hopping Methods Against Accurate Quantum Mechanical Dynamics and Semiclassical Analysis of Electronic-to-Vibrational Energy Transfer", J. Chem. Phys. **106**, 8699 (1997).

[14] M. S. Topaler, T. C. Allison, D. W. Schwenke and D. G. Truhlar, "Test of Trajectory Surface Hopping Against Accurate Quantum Dynamics for an Electronically Nonadiabatic Chemical Reaction", J. Phys. Chem. A **102**, 1666 (1998).

[15] M. S. Topaler, T. C. Allison, D. W. Schwenke and D. G. Truhlar, "What is the Best Semiclassical Method for Photochemical Dynamics in Systems with Conical Intersections?", J. Chem. Phys., in press, (1998).

[16] Y. L. Volobuev and D. G. Truhlar, "Four-body Quantum Dynamics on the Nanosecond Time Scale: Lifetime of Photoexcited HF Dimer", to be published.

[17] Y. Volobuev, W. C. Necoechea and D. G. Truhlar, "Tunneling Splittings in Predissociated HF Dimer", J. Phys. Chem. **101**, 3045 (1997).

[18] D. Thirumalai, T. C. Thompson and D. G. Truhlar, "Rational Fraction Analytic Continuation Method for Complex Resonance Energies in Multi-dimensional Systems", J. Chem. Phys. **80**, 5864 (1984).

R. Prosmiti, J. Tennyson, D. C. Clary (eds.)
Molecular Quantum States at Dissociation

Semiclassical Theory of Electronically Nonadiabatic Processes

William H. Miller
Department of Chemistry, University of California, and
Chemical Sciences Division, Lawrence Berkeley National Laboratory,
Berkeley, California 94720, USA

The semiclassical (SC) initial value representation (IVR) [1–6] is currently receiving a great deal of attention as a way of including quantum interference and tunnelling effects in molecular dynamics simulations. This is essentially the traditional SC approximation [7] cast in a form that requires one to integrate classical trajectories specified by their initial conditions (rather than by double-ended boundary conditions); e.g., a matrix element of the time evolution operator has the form

$$\langle \psi_f | e^{-i\hat{H}t/\hbar} | \psi_i \rangle = \int d\boldsymbol{p}_0 \int d\boldsymbol{q}_0 \sqrt{\left| \frac{\partial \boldsymbol{q}_t}{\partial \boldsymbol{p}_0} \right| / (2\pi i\hbar)^F}\, e^{iS_t(\boldsymbol{p}_0,\boldsymbol{q}_0)/\hbar} \psi_f(\boldsymbol{q}_t)^* \psi_i(\boldsymbol{q}_0), \tag{1a}$$

where $\boldsymbol{q}_t \equiv \boldsymbol{q}_t(\boldsymbol{p}_0, \boldsymbol{q}_0)$ is the coordinate at time t for the trajectory with initial conditions $(\boldsymbol{p}_0, \boldsymbol{q}_0)$, and S_t is the action integral along it. Eq. (1a) can be expressed more abstractly as

$$e^{-i\hat{H}t/\hbar} = \int d\boldsymbol{p}_0 \int d\boldsymbol{q}_0 \sqrt{\left| \frac{\partial \boldsymbol{q}_t}{\partial \boldsymbol{p}_0} \right| / (2\pi i\hbar)^F}\, e^{iS_t(\boldsymbol{p}_0,\boldsymbol{q}_0)/\hbar} |\boldsymbol{q}_t\rangle\langle \boldsymbol{q}_0|, \tag{1b}$$

and there is also a coherent state version [3] of this same form that is sometimes more useful. Eq. (1) can be used to construct a semiclassical approximation for any quantum dynamical property that is expressed in terms of the time evolution operator, e.g., S-matrix elements for scattering processes, eigenvalues of bound molecular systems, or time correlation functions that describe various average dynamical quantities.

Of the many applications of the SC-IVR approach, one of the most interesting is to *electronically non-adiabatic* processes [8–10]. This is based on the classical model that Meyer and Miller [11] (MM) introduced some years ago for representing a finite set of electronic states by classical degrees of freedom, so that the electronic and nuclear dynamics could be treated on an equivalent basis. In the Cartesian representation for these classical electronic degrees of freedom, this approach gives the following classical Hamiltonian for the electronic $(\boldsymbol{x}, \boldsymbol{p}) \equiv \{x_i, p_i\}, i = 1 \ldots N$ and nuclear $(\boldsymbol{Q}, \boldsymbol{P})$ degrees of freedom (assumed for simplicity to be Cartesian)

$$H(\boldsymbol{x}, \boldsymbol{p}, \boldsymbol{Q}, \boldsymbol{P}) = \frac{\boldsymbol{P}^2}{2\mu} + H_{\mathrm{el}}(\boldsymbol{x}, \boldsymbol{p}; \boldsymbol{Q}), \tag{2a}$$

with

$$H_{\mathrm{el}}(\boldsymbol{x}, \boldsymbol{p}; \boldsymbol{Q}) = \sum_{i=1}^{N} H_{i,i}(\boldsymbol{Q}) \frac{1}{2}(x_i^2 + p_i^2 - 1) + \sum_{i<j=1}^{N} H_{i,j}(\boldsymbol{Q})(x_i x_j + p_i p_j), \tag{2b}$$

where $H_{i,j}(\boldsymbol{Q})$ is a diabatic electronic Hamiltonian matrix that depends parametrically on nuclear coordinates $\boldsymbol{Q}$ and is assumed to come from a quantum mechanical electronic structure calculation. (Stock and Thoss [9] have recently shown that this Hamiltonian can also be obtained by extending Schwinger's angular momentum formalism to the N-level case.) MM used this Hamiltonian to carry out classical trajectory simulations, treating electronic and nuclear degrees of freedom on the same footing; i.e., the initial conditions for the nuclear and electronic degrees of freedom are both sampled by the standard "quasiclassical" prescription (integer values for the initial action variables and random angle variables), histogramming the final action variables to obtain final electronic and nuclear quantum states. A variety of applications using this model were quite successful [12]. The present interest, though, is to upgrade the description of both electronic and nuclear degrees of freedom to the semiclassical level, using the SC-IVR; i.e., one still integrates electronic-nuclear trajectories from the MM Hamiltonian of Eq. (2), but uses them in Eq. (1). (MM [11], in fact, also noted that the model could be implemented semiclassically and gave some results of this using "classical S-matrix" theory, [7][a] i.e., the stationary phase limit of the SC-IVR.) All that is needed to apply Eq. (1) are the initial and final electronic-nuclear wavefunctions, which are of the form

$$\psi_{i,n}(\boldsymbol{x}, \boldsymbol{Q}) = \phi_i(\boldsymbol{x}) \chi_n(\boldsymbol{Q}); \tag{3}$$

$\chi_n(\boldsymbol{Q})$ is the nuclear wavefunction, and the electronic wavefunction for state i is

$$\phi_i(\boldsymbol{x}) = \phi_1(x_i) \prod_{j=1, j\neq i}^{N} \phi_0(x_j), \tag{4a}$$

where $\phi_0(x)$ and $\phi_1(x)$ are the ground and first excited harmonic oscillator wavefunctions, respectively; thus one has the specific form

$$\Phi_i(\boldsymbol{x}) = \sqrt{2} \left(\frac{1}{\pi}\right)^{N/4} x_i \exp\left[-\sum_{k=1}^{N} \frac{1}{2} x_k^2 \right]. \tag{4b}$$

The model of the electronic degrees of freedom is thus that of a harmonic oscillator for each electronic state; the ith electronic state corresponds to one vibrational quantum in the ith mode, with all the other modes being in their ground state. Though the construction of this nuclear-electronic Hamiltonian in Eq. (2) was motivated by the desire to have a *classical* model that treated the electronic and nuclear dynamics on an equal footing, it is important to note that the quantum mechanical Hamiltonian operator corresponding to Eq. (2) is an *exact* representation of the *quantum* electronic-nuclear dynamical system. This is easy to see because the matrix of the "electronic" Hamiltonian operator $\hat{H}_{\rm el}$ of Eq. (2b),

$$\hat{H}_{\rm el} \equiv \sum_{i=1}^{N} H_{i,i}(\boldsymbol{Q})\frac{1}{2}(\hat{x}_i^2 + \hat{p}_i^2 - 1) + \sum_{i<j=1}^{N} H_{i,j}(\boldsymbol{Q})(\hat{x}_i\hat{x}_j + \hat{p}_i\hat{p}_j), \tag{5}$$

in the basis $\{\Phi_i(\boldsymbol{x})\}$ of Eq. (4) is the original diabatic electronic matrix, i.e.,

$$\langle\Phi_i|\hat{H}_{\rm el}|\Phi_j\rangle = H_{i,j}(\boldsymbol{Q}), \tag{6}$$

as can be easily verified by using standard harmonic oscillator matrix elements. The SC-IVR version of the MM model has been applied to the three non-adiabatic scattering problems Tully [13] used to test his fewest switches version of the surface hopping model, with very good agreement with the correct quantum results. This includes a case involving Stuekelberg oscillations, i.e., interference effects between non-adiabatic transitions at different times. It has most recently [10] been applied to the spin-boson problem — a two state system coupled to an infinite bath of harmonic oscillators — which is often used as a model of non-adiabatic transitions in a condensed phase. The SC-IVR description is in excellent agreement with accurate quantum results (Feynman path integral calculations by Mak and Chandler [14] and by Makarov and Makri [15]), including both the coherent (weak coupling) and incoherent (strong coupling) regimes, and the transition between them. The SC-IVR is thus emerging as a comprehensive approach that is able to describe quantum effects in a wide range of molecular dynamics simulations.

ACKNOWLEDGMENTS

This work has been supported by the Director, Office of Energy Research, Office of Basic Energy Sciences, Chemical Sciences Division of the U.S. Department of Energy under contract No. DE-AC03-76SF00098, by the Laboratory Directed Research and Development (LDRD) project from the National Energy Research Scientific Computing (NERSC) Center, Lawrence Berkeley National Laboratory, and also by the National Science Foundation under Grant No. CHE9732758.

[1] W.H. Miller, J. Chem. Phys. **53**, 3578(1970).
[2] (a) E.J. Heller, J. Chem. Phys. **94**, 2723 (1991); (b) W.H. Miller, ibid. **95**, 9428 (1991); (c) E.J. Heller, ibid. **95**, 9431 (1991).
[3] (a) K.G. Kay, J. Chem. Phys. **100** 4377 (1994); **100** 4432 (1994); **101** 2250 (1994); (b) M.F. Herman and E. Kluk, Chem. Phys. **91**, 27 (1984); (c) E. Kluk, M.F. Herman and H.L. Davis, J. Chem. Phys. **84**, 326 (1986); (d) A.R. Walton and D.E. Manolopoulos, Mol. Phys. **87**, 961 (1996); (e) M.L. Brewer, J.S. Hume and D.E. Manolopoulos, J. Chem. Phys. **106**, 4832 (1997).
[4] (a) D. Provost and P. Brumer, Phys. Rev. A **74**, 250 (1995); (b) G. Campolieti and P. Brumer, Phys. Rev. A **50**, 997 (1994); (c) G. Campolieti and P. Brumer, J. Chem. Phys. **96**, 5969 (1992); (d) G. Campolieti and P. Brumer, ibid. **107**, 791 (1997).
[5] (a) S. Keshavamurthy and W.H. Miller, Chem. Phys. Lett. **218** 189 (1994); (b) S. Garashchuk and D.J. Tannor, ibid. **262**, 477 (1996); (c) F. Grossmann, ibid. **262**, 470 (1996); (d) K.G. Kay, J. Chem. Phys. **107**, 2313 (1997); (e) N.T. Maitra and E.J. Heller, Phys. Rev. Lett. **78** 3035 (1997).
[6] (a) B.W. Spath and W.H. Miller, Chem. Phys. Lett. **262**, 486 (1996); (b) A.R. Walton and D.E. Manolopoulos, Chem. Phys. Lett. **244**, 448 (1995).
[7] (a) W.H. Miller, Adv. Chem. Phys. **25**, 69 (1974); (b) M. S. Child, *Semiclassical Mechanics with Molecular Applications*, (Oxford University Press, Oxford, 1991).
[8] X. Sun and W.H. Miller, J. Chem. Phys. **106**, 6346 (1997).
[9] G. Stock and M. Thoss, Phys. Rev. Lett. **78**, 578 (1997).
[10] X. Sun, H. B. Wang and W.H. Miller, J. Chem. Phys. in press, (1998).
[11] (a) H.D. Meyer and W.H. Miller, J. Chem. Phys. **70**, 3214 (1979); (b) H.D. Meyer and W.H. Miller, J. Chem. Phys. **71**, 2156 (1979).
[12] (a) H.D. Meyer and W.H. Miller, J. Chem. Phys. **72**, 2272 (1980); (b) A.E. Orel and W.H. Miller, ibid. **73**, 241 (1980); (c) A.E. Orel, D.P. Ali and W.H. Miller, Chem. Phys. Lett. **79**, 137 (1981); (d) W.H. Miller and A.E. Orel, J. Chem. Phys. **74**, 6075 (1981); (e) S.K. Gray and W.H. Miller, Chem. Phys. Lett. **93**, 341 (1982); (f) D.P. Ali and W.H. Miller, ibid. **103**, 470 (1984).
[13] J.C. Tully, J. Chem. Phys. **93**, 1061 (1990).
[14] C.H. Mak and D. Chandler, Phys. Rev. A **44**, 2352 (1991).
[15] D.E. Makarov and N. Makri, Chem. Phys. Lett. **221**, 482 (1994).